

Studies of the motion and decay of axion walls bounded by strings.

S. Chang¹, C. Hagmann² and P. Sikivie¹

¹*Department of Physics, University of Florida, Gainesville, FL 32611*

²*Lawrence Livermore National Laboratory, Livermore, CA 94550*

(November 7, 2018)

Abstract

We discuss the appearance at the QCD phase transition, and the subsequent decay, of axion walls bounded by strings in $N = 1$ axion models. We argue on intuitive grounds that the main decay mechanism is into barely relativistic axions. We present numerical simulations of the decay process. In these simulations, the decay happens immediately, in a time scale of order the light travel time, and the average energy of the radiated axions is $\langle\omega_a\rangle \simeq 7m_a$ for $v_a/m_a \simeq 500$. $\langle\omega_a\rangle$ is found to increase approximately linearly with $\ln(v_a/m_a)$. Extrapolation of this behaviour yields $\langle\omega_a\rangle \sim 60 m_a$ in axion models of interest. We find that the contribution to the cosmological energy density of axions from wall decay is of the same order of magnitude as that from vacuum realignment, with however large uncertainties. The velocity dispersion of axions from wall decay is found to be larger, by a factor 10^3 or so, than that of axions from vacuum realignment and string decay. We discuss the implications of this for the formation and evolution of axion miniclusters and for the direct detection of axion dark matter on Earth. Finally we discuss the cosmology of axion models with $N > 1$ in which the domain wall problem is solved by introducing a small $U_{PQ}(1)$ breaking interaction. We find that in this case the walls decay into gravitational waves.

PACS numbers:14.80.Mz,95.30.Cq

I. INTRODUCTION

The axion [1,2] was postulated approximately twenty years ago to explain why the strong interactions conserve the discrete symmetries P and CP in spite of the fact that the Standard Model of particle interactions as a whole violates those symmetries. It is the quasi-Nambu-Goldstone boson associated with the spontaneous breaking of a $U_{PQ}(1)$ symmetry which Peccei and Quinn postulated. At zero temperature the axion mass is given by:

$$m_a \simeq 6 \cdot 10^{-6} \text{eV} \cdot N \cdot \left(\frac{10^{12} \text{GeV}}{v_a} \right) \quad (1.1)$$

where v_a is the magnitude of the vacuum expectation value that breaks $U_{PQ}(1)$ and N is a strictly positive integer that describes the color anomaly of $U_{PQ}(1)$. Axion models have N degenerate vacua [3,2]. Searches for the axion in high energy and nuclear physics experiments have only produced negative results. By combining the constraints from these experiments with those from astrophysics [2,4], one obtains the following bound: $m_a \lesssim 10^{-2}$ eV.

The axion owes its mass to non-perturbative QCD effects. In the very early universe, at temperatures high compared to the QCD scale, these effects are suppressed [5] and the axion mass is negligible. The axion mass turns on when the temperature approaches the QCD scale and increases till it reaches the value given in Eq.(1.1) which is valid below the QCD scale. There is a critical time t_1 , defined by $m_a(t_1)t_1 = 1$, when the axion mass effectively turns on [6]. The corresponding temperature $T_1 \simeq 1$ GeV.

The implications of the existence of an axion for the history of the early universe may be briefly described as follows. At a temperature of order v_a , a phase transition occurs in which the $U_{PQ}(1)$ symmetry becomes spontaneously broken. This is called the PQ phase transition. At that time axion strings appear as topological defects. One must distinguish two cases: 1) inflation occurs with reheat temperature higher than the PQ transition temperature (equivalently, for the purposes of this paper, inflation does not occur at all) or 2) inflation occurs with reheat temperature less than the PQ transition temperature.

In case 2) the axion field gets homogenized by inflation and the axion strings are ‘blown away’. When the axion mass turns on at t_1 , the axion field starts to oscillate. The amplitude of this oscillation is determined by how far from zero the axion field is when the axion mass turns on. The axion field oscillations do not dissipate into other forms of energy and hence contribute to the cosmological energy density today [6]. Such a contribution is called of “vacuum realignment”. Note that the vacuum realignment contribution may be accidentally suppressed in case 2) because the axion field, which has been homogenized by inflation, may happen to lie close to zero.

In case 1) the axion strings radiate axions [7,8] from the time of the PQ transition till t_1 when the axion mass turns on. At t_1 each string becomes the boundary of N domain walls. If $N = 1$, the network of walls bounded by strings is unstable [9,10] and decays away. All of the present paper except section VI is concerned with this process, how many axions are produced in the decay, what is the velocity dispersion of these axions and what are the implications.

If $N > 1$ there is a domain wall problem [3] because axion domain walls end up dominating the energy density, resulting in a universe very different from the one observed today. There is a way to avoid the domain wall problem by introducing an interaction which slightly

lowers one of the N vacua with respect to the others. In that case, the lowest vacuum takes over after some time and the domain walls disappear. There is little room in parameter space for that to happen but it is a logical possibility. Section VI discusses this in detail.

In case 1) there are three contributions to the axion cosmological energy density. One contribution [7,8,11,12] is from axions that were radiated by axion strings before t_1 ; let us call it the string decay contribution. A second contribution is from axions that were produced in the decay of walls bounded by strings after t_1 [12–14]; call it the contribution from wall decay. A third contribution is from vacuum realignment [6]. To convince oneself that there is a vacuum realignment contribution distinct from the other two, consider a region of the universe which happens to be free of strings and domain walls. In such a region the axion field is generally different from zero, even though no strings or walls are present. After time t_1 , the axion field oscillates implying a contribution to the energy density which is neither from string decay nor wall decay. Since the axion field oscillations caused by vacuum realignment, string decay and wall decay are mutually incoherent, the three contributions to the energy density should simply be added to each other [12].

That axions walls bounded by strings decay predominantly into barely relativistic axions was suggested in ref. [12], where the size of the wall contribution to the axion energy density was estimated to be of the same order of magnitude as that from string decay and from vacuum realignment. This is consistent with what we find here. D. Lyth [13] also discussed the wall decay contribution and emphasized the uncertainties affecting it. M. Nagasawa and M. Kawasaki [14] performed computer simulations of the decay of walls bounded by string and obtained $\langle\omega_a\rangle/m_a \simeq 3$ for the average energy of the radiated axions. Our simulations, presented in section IV, are similar to those of Nagasawa and Kawasaki but they are done on larger lattices and for a wider variety of initial conditions. We obtain $\langle\omega_a\rangle/m_a \simeq 7$ for $v_a/m_a \simeq 500$. We attribute the difference between our result and that of Nagasawa and Kawasaki to the fact that we give angular momentum to the collapsing walls, whereas they did not.

It should be emphasized that the lattice sizes which are amenable to present day computers are at any rate small compared to what one would ideally wish. Indeed the axion string core has size of order $\frac{1}{\sqrt{\lambda}v_a}$ where λ is a coupling constant (see section II) whereas the axion domain wall thickness is of order m_a^{-1} . The lattice constant must be smaller than $\frac{1}{\sqrt{\lambda}v_a}$ for the lattice to resolve the string core. On the other hand the lattice size must be larger than m_a^{-1} to contain at least one wall. Hence the lattice size in units of the lattice constant must be of order $10\frac{\sqrt{\lambda}v_a}{m_a} \times 10\frac{\sqrt{\lambda}v_a}{m_a}$ or larger if the simulations are done in 2 dimensions (see section IV). Present day computers allow lattice sizes of order 4000×4000 , i.e. $\frac{\sqrt{\lambda}v_a}{m_a} \sim 100$. In axion models of interest $\frac{\sqrt{\lambda}v_a}{m_a} \sim \frac{10^{12}\text{GeV}}{10^{-5}\text{eV}} = 10^{26}$. The computer simulations inform us about the situation of interest only insofar it may be assumed that the motion and decay of walls bounded by strings do not vary dramatically from the case where $\frac{v_a}{m_a}$ is large to the case where $\frac{v_a}{m_a}$ is huge. To address this issue, we study the dependence of $\langle\omega_a\rangle/m_a$ upon the $\frac{\sqrt{\lambda}v_a}{m_a}$ and find that it increases approximately as the logarithm of that quantity over the range accessible to the simulations. This behaviour is understood in terms of the process by which the walls bounded by string decay. If it persists all the way up to $\frac{\sqrt{\lambda}v_a}{m_a} = 10^{26}$, then $\langle\omega_a\rangle/m_a$ is of order 60 in models of interest.

There has been disagreement in the literature about the size of the string contribution.

Many authors [7,11] believe it is about a factor 100 larger than the vacuum realignment contribution. We ourselves [8,12] have argued that the string and vacuum realignment contributions are of the same order of magnitude. The two different estimates are presented in subsection IIIB. With regard to the wall contribution, we argue that it is again of the same order of magnitude as that from vacuum realignment, with however large uncertainties. Section III presents a unified treatment of all contributions. The resulting axion cosmological energy density is obtained in subsection IIID. The requirement that it does not overclose the universe, implies $m_a \gtrsim 10^{-6}$ eV. By combining this bound with the one from stellar evolution mentioned earlier, the axion mass is constrained to lie in the window: $10^{-2}\text{eV} \gtrsim m_a \gtrsim 10^{-6}$ eV.

We find that the velocity dispersion of the axions from wall decay is much larger, by a factor of 10^3 or so, than the velocity dispersion of the axions from string decay and vacuum realignment. This has interesting implications for the formation and evolution of axion mini-clusters [16,17] as discussed in section V. We find that the axions from wall decay bind only very loosely to axion mini-clusters and that they get readily stripped off when the mini-cluster falls into a galactic halo. This ensures the existence of an unclustered component of galactic axion dark matter. The existence of such a component is important for searches of axion dark matter on Earth [18] because it guarantees that the signal is on at all times.

Another interesting consequence of the larger velocity dispersion of the axions from wall decay is that it may conceivably be measured. If a signal is found in the cavity detector of dark matter axions [18], the energy spectrum of these axions can be measured with great resolution. It has been pointed out that there are peaks in the spectrum [19] because late infall of cold dark matter onto our galaxy produces distinct flows, each one with a characteristic local velocity vector. These peaks are broadened by the primordial velocity dispersion. The minimum time required to measure the primordial velocity dispersion of axions from vacuum realignment and string decay is too long (~ 10 years) to be practical, but the minimum time required to measure that of axions from wall decay is much less. This is discussed in subsection IIIE.

This paper is organized as follows. In section II, we present a toy model which captures all the physics we are interested in. We discuss the evolution of axion strings in the early universe and the formation of walls bounded by strings at the onset of the QCD phase transition. We give an estimate of the density of walls at that time. In section III, we discuss the decay of walls bounded by string and the axion population that results therefrom. We also discuss the axions from vacuum realignment and from string decay and estimate the total cosmological energy density from these mechanisms. In section IV, we present our numerical simulations of the motion and decay of walls bounded by strings. In section V, we discuss the effect of axions from wall decay upon the formation and evolution of axion miniclusters. In section VI, we discuss axion models in which $N > 1$ and in which the axion domain wall problem is solved by slightly lowering one of the N vacua with respect to the others. In section VII, we summarize our conclusions.

II. THE NETWORK OF WALLS BOUNDED BY STRINGS

The bulk of this paper is concerned with the cosmological properties of $N = 1$ axion models. $N = 1$ means that the axion model has a unique vacuum. The following toy model

incorporates the qualitative features of interest to us:

$$\begin{aligned}\mathcal{L} &= \frac{1}{2}\partial_\mu\phi^\dagger\partial^\mu\phi - \frac{\lambda}{4}(\phi^\dagger\phi - v_a^2)^2 + \eta v_a\phi_1 \\ &= \frac{1}{2}\partial_\mu\phi_1\partial^\mu\phi_1 + \frac{1}{2}\partial_\mu\phi_2\partial^\mu\phi_2 - \frac{\lambda}{4}(\phi_1^2 + \phi_2^2 - v_a^2)^2 + \eta v_a\phi_1\end{aligned}\quad (2.1)$$

where $\phi = \phi_1 + i\phi_2$ is a complex scalar field. When $\eta = 0$, this model has a $U(1)$ global symmetry under which $\phi(x) \rightarrow e^{i\alpha}\phi(x)$. It is analogous to the $U_{PQ}(1)$ symmetry of Peccei and Quinn. It is spontaneously broken by the vacuum expectation value $\langle\phi\rangle = v_a e^{i\alpha}$. The associated Nambu-Goldstone boson is the axion. The last term in Eq. (2.1) represents the non-perturbative QCD effects that give the axion its mass m_a . We have $m_a = \sqrt{\eta}$ for $v_a \gg m_a$.

When $\eta = 0$, the model has global string solutions. A straight global string along the \hat{z} -axis is the static configuration:

$$\phi(\vec{x}) = v_a f(\rho) e^{i\theta} \quad (2.2)$$

where (z, ρ, θ) are cylindrical coordinates and $f(\rho)$ is a function which goes from zero at $\rho = 0$ to one at $\rho = \infty$ over a distance scale of order $\delta \equiv (\sqrt{\lambda}v_a)^{-1}$. $f(\rho)$ may be determined by solving the non-linear field equations derived from Eq. (2.1). The energy per unit length of the global string is

$$\mu \simeq 2\pi \int_\delta^L \rho d\rho \frac{1}{2} |\vec{\nabla}\phi|^2 = \pi v_a^2 \ln(\sqrt{\lambda}v_a L) \quad (2.3)$$

where L is a long-distance cutoff. Eq. (2.3) neglects the energy per unit length, of order v_a^2 , associated with the core of the string. For a network of strings with random directions, as would be present in the early universe, the infra-red cutoff L is of order the distance between strings.

When $\eta \neq 0$, the model has domain walls. If $v_a \gg m_a$ we may set $\phi(x) = v_a e^{\frac{i}{v_a}a(x)}$ when restricting ourselves to low energy configurations. The corresponding effective Lagrangian is :

$$\mathcal{L}_a = \frac{1}{2}\partial_\mu a\partial^\mu a + m_a^2 v_a^2 \left[\cos\left(\frac{a}{v_a}\right) - 1 \right]. \quad (2.4)$$

Its equation of motion has the well-known Sine-Gordon soliton solution :

$$\frac{a(y)}{v_a} = 2\pi n + 4 \tan^{-1} \exp(m_a y) \quad (2.5)$$

where y is the coordinate perpendicular to the wall and n is any integer. Eq. (2.5) describes a domain wall which interpolates between neighboring vacua in the low energy effective theory (2.4). In the original theory (2.1), the domain wall interpolates between the unique vacuum back to that same vacuum going around the bottom of the Mexican hat potential $V(\phi^\dagger\phi) = \frac{\lambda}{4}(\phi^\dagger\phi - v_a^2)^2$ once.

The thickness of the wall is of order m_a^{-1} . The wall energy per unit surface is $\sigma = 8m_a v_a^2$ in the toy model. In reality the structure of axion domain walls is more complicated than

in the toy model, mainly because not only the axion field but also the neutral pion field is spatially varying inside the wall [20]. When this is taken into account, the (zero temperature) wall energy/surface is found to be:

$$\sigma \simeq 4.2 f_\pi m_\pi f_a \simeq 9 m_a f_a^2 \quad (2.6)$$

with $f_a \equiv v_a/N$. For $N = 1$, f_a and v_a are the same. However, written in terms of f_a , Eq. (2.6) is valid for $N \neq 1$ also.

When $m_a \neq 0$, each string becomes the boundary of a domain wall. Indeed the presence of the string forces $\alpha(\vec{x}) = \frac{1}{v_a} a(\vec{x})$ to vary by 2π when \vec{x} goes around the string once and a domain wall is the minimum energy path that does this. Fig. 1 shows a cross-section of a wall bounded by a string. Two different length scales are involved: the wall thickness m_a^{-1} and the string core size $\delta = (\sqrt{\lambda} v_a)^{-1}$. Walls bounded by string are of course topologically unstable.

In the early universe, the axion is essentially massless from the PQ phase transition at temperature of order v_a to the QCD phase transition at temperature of order 1 GeV. During that epoch, axion strings are present as topological defects. At first the strings are stuck in the plasma and are stretched by the Hubble expansion. However with time the plasma becomes more dilute and below temperature [8]

$$T_* \sim 2 \cdot 10^7 \text{GeV} \left(\frac{v_a}{10^{12} \text{GeV}} \right)^2 \quad (2.7)$$

the strings move freely and decay efficiently into axions. Because this decay mechanism is very efficient, there is approximately one string per horizon from temperature T_* to temperature $T_1 \simeq 1$ GeV when the axion acquires mass. The decay of axion strings into axions has been discussed extensively in the literature and is reviewed in subsection III B.

At temperature T_1 each string becomes the boundary of a domain wall. Walls not bounded by string are also present. We want to obtain statistical properties of this network of walls and strings under the assumption that the axion field is randomly oriented from one horizon to the next just before the axion mass turns on at time t_1 . In particular: What are the average densities of walls and of strings? Are there walls of infinite extent which are not cut up by any string? What is the energy fraction in walls not cut up by string?

To address such questions, a cross-section of a finite but statistically significant volume of the universe near time t_1 was simulated in the following manner [10]. A 2-dim. hexagonal grid was constructed. Each hexagon represents a causally disconnected region. The circle $\{\langle \phi \rangle = v_a e^{i\alpha} : -\pi < \alpha = \frac{a}{v_a} \leq +\pi\}$ is divided into three equal parts as shown in Fig. 2a. $\alpha = 0$ is at the middle of part 1. $\alpha = \pi$ is at the boundary between parts 2 and 3. Each hexagon is then randomly assigned a number 1, 2 or 3. A hexagon to which #1 is assigned is thought of as a horizon volume in which the average value of α is in part 1 of the circle, and so on. Thus there is a domain wall at each boundary between two hexagons one of which has been assigned #2 and the other #3. Likewise there is an downward-going string at each vertex surrounded by hexagons to which #1, #2 and #3 have been assigned in clockwise order, and an upward-going string at each vertex surrounded by hexagons to which #1, #2 and #3 have been assigned in counter-clockwise order. Fig. 2b shows some examples. Fig. 3 shows a larger realization with the underlying grid removed.

Fig. 3 shows that there are no infinite domain walls which are not cut up by any string. The reason for this is simple. An extended domain wall has some probability to be cut up by string in each successive horizon it traverses. The probability that no string is encountered after traveling a distance l along the wall decreases exponentially with l . Fig. 3 also shows that finite domain walls which are not cut up by string, and which therefore close onto themselves like a sphere or a donut, are very rare. Indeed, the figure shows only one closed circle and a circle need not be a section of a sphere; it could be a section of a tube. The average density of walls at time t_1 predicted by the random process described here is approximately $2/3$ per horizon volume. This is consistent with Fig. 3.

III. THE COLD AXION POPULATIONS.

In this section, we discuss the various contributions to the cosmological energy density in the form of *cold* axions. In addition to cold axions, there is a thermal axion population whose properties are derived by the usual application of statistical mechanics to the early, high temperature universe [15]. The contribution of thermal axions to the cosmological energy density is subdominant if $m_a \lesssim 10^{-2}$ eV. We concern ourselves only with cold axions here.

We distinguish the following sources of cold axions:

1. vacuum realignment
 - a. “zero momentum” mode
 - b. higher momentum modes
2. axion string decay
3. axion domain wall decay

The basis for distinguishing the contribution from vacuum realignment from the other two is that it is present for any quasi-Nambu-Goldstone field regardless of the topological structures associated with that field. Contributions 1a and 1b are distinguished by whether the misalignment of the axion field from the CP conserving direction is in modes of wavelength larger (1a) or shorter (1b) than the horizon size t_1 at the moment the axion mass turns on. Contribution 2 is from the decay of axion strings before the QCD phase transition. Contribution 3 is from the decay of axion domain walls bounded by strings after the QCD phase transition. In the past literature on the axion cosmological energy density, contributions 1a and 2 have been discussed in detail whereas contributions 1b and 3 have received much less attention. This section presents a systematic analysis of all contributions.

A. Vacuum realignment

Let us track the axion field from the PQ phase transition, when $U_{PQ}(1)$ gets spontaneously broken and the axion appears as a Nambu-Goldstone boson, to the QCD phase transition when the axion acquires mass. For clarity of presentation we consider in this subsection a large region which happens to be free of axion strings. Although such a region is rare in practice it may exist in principle. In it, the contribution to the cosmological axion energy density from string and domain wall decay vanishes but that from vacuum realignment does not. In more typical regions where strings are present, the contributions from

string and domain wall decay should simply be added to that from vacuum realignment.

In the radiation dominated era under consideration, the space-time metric is given by:

$$- ds^2 = -dt^2 + R^2(t) d\vec{x} \cdot d\vec{x} \quad (3.1)$$

where t is the age of the universe, \vec{x} are co-moving coordinates and $R(t) \sim \sqrt{t}$ is the scale factor. The axion field $a(x)$ satisfies:

$$\left(D_\mu D^\mu + m_a^2(t) \right) a(x) = \left(\partial_t^2 + 3\frac{\dot{R}}{R}\partial_t - \frac{1}{R^2}\nabla_x^2 + m_a^2(t) \right) a(x) = 0 \quad (3.2)$$

where $m_a(t) = m_a(T(t))$ is the time-dependent axion mass. We will see that the axion mass is unimportant as long as $m_a(t) \ll 1/t$, a condition which is satisfied throughout except at the very end when t approaches t_1 . The solution of Eq. (3.2) is a linear superposition of eigenmodes with definite co-moving wavevector \vec{k} :

$$a(\vec{x}, t) = \int d^3k a(\vec{k}, t) e^{i\vec{k}\cdot\vec{x}} \quad (3.3)$$

where the $a(\vec{k}, t)$ satisfy:

$$\left(\partial_t^2 + \frac{3}{2t}\partial_t + \frac{k^2}{R^2} + m_a^2(t) \right) a(\vec{k}, t) = 0. \quad (3.4)$$

Eqs. (3.1) and (3.3) show that the wavelength $\lambda(t) = \frac{2\pi}{k}R(t)$ of each mode is stretched by the Hubble expansion. There are two qualitatively different regimes in the evolution of each mode depending on whether its wavelength is outside ($\lambda(t) > t$) or inside ($\lambda(t) < t$) the horizon.

For $\lambda(t) \gg t$, only the first two terms in Eq. (3.4) are important and the most general solution is:

$$a(\vec{k}, t) = a_0(\vec{k}) + a_{-1/2}(\vec{k})t^{-1/2}. \quad (3.5)$$

Thus, for wavelengths larger than the horizon, each mode goes to a constant; the axion field is so-called ‘‘frozen by causality’’.

For $\lambda(t) \ll t$, the first three terms in Eq. (3.4) are important. Let $a(\vec{k}, t) = R^{-\frac{3}{2}}(t)\psi(\vec{k}, t)$. Then

$$\left(\partial_t^2 + \omega^2(t) \right) \psi(\vec{k}, t) = 0 \quad (3.6)$$

where

$$\omega^2(t) = m_a^2(t) + \frac{k^2}{R^2(t)} + \frac{3}{16t^2} \simeq \frac{k^2}{R^2(t)}. \quad (3.7)$$

Since $\dot{\omega} \ll \omega^2$, this regime is characterized by the adiabatic invariant $\psi_0^2(\vec{k}, t)\omega(t)$, where $\psi_0(\vec{k}, t)$ is the oscillation amplitude of $\psi(\vec{k}, t)$. Hence the most general solution is:

$$a(\vec{k}, t) = \frac{A}{R(t)} \cos \left(\int^t dt' \omega(t') \right). \quad (3.8)$$

The energy density and the number density behave respectively as $\rho_{a,\vec{k}} \sim \frac{A^2 \omega^2}{R^2(t)} \sim \frac{1}{R^4(t)}$ and $n_{a,\vec{k}} \sim \frac{1}{\omega} \rho_{a,\vec{k}} \sim \frac{1}{R^3(t)}$, indicating that the number of axions in each mode is conserved. This is as expected because the expansion of the universe is adiabatic for $\lambda(t)t \ll 1$.

Let us define $\frac{dn_a}{d\omega}(\omega, t)$ to be the number density, in physical and frequency space, of axions with wavelength $\lambda = \frac{2\pi}{\omega}$, for $\omega > t^{-1}$. The axion number density in physical space is thus:

$$n_a(t) = \int_{t^{-1}} d\omega \frac{dn_a}{d\omega}(\omega, t), \quad (3.9)$$

whereas the axion energy density is:

$$\rho_a(t) = \int_{t^{-1}} d\omega \frac{dn_a}{d\omega}(\omega, t) \omega. \quad (3.10)$$

Under the Hubble expansion axion energies redshift according to $\omega' = \omega \frac{R}{R'}$, and volume elements expand according to $\Delta V' = \Delta V \left(\frac{R'}{R}\right)^3$, whereas the number of axions is conserved mode by mode. Hence:

$$\frac{dn_a}{d\omega}(\omega, t) = \left(\frac{R'}{R}\right)^2 \frac{dn_a}{d\omega}\left(\omega \frac{R}{R'}, t'\right). \quad (3.11)$$

Moreover, the size of $\frac{dn_a}{d\omega}$ for $\omega \sim \frac{1}{t}$ is determined in order of magnitude by the fact that the axion field typically varies by f_a from one horizon to the next. Thus:

$$\omega \frac{dn_a}{d\omega}(\omega, t) \Delta\omega \Big|_{\omega \sim \Delta\omega \sim \frac{1}{t}} \sim \frac{dn_a}{d\omega}\left(\frac{1}{t}, t\right) \left(\frac{1}{t}\right)^2 \sim \frac{1}{2} (\vec{\nabla} a)^2 \sim \frac{1}{2} \frac{f_a^2}{t^2}. \quad (3.12)$$

From Eqs. (3.11) and (3.12), and $R \sim \sqrt{t}$, we have:

$$\frac{dn_a}{d\omega}(\omega, t) \sim \frac{f_a^2}{2t^2 \omega^2}. \quad (3.13)$$

Eq. (3.13) holds until the moment the axion acquires mass during the QCD phase transition. The critical time is when $m_a(t)$ is of order t^{-1} . Let us define t_1 :

$$m_a(t_1)t_1 = 1. \quad (3.14)$$

$m_a(T)$ was obtained [6] from a calculation of the effects of QCD instantons at high temperature [5]:

$$m_a(T) \simeq 4 \cdot 10^{-9} \text{eV} \left(\frac{10^{12} \text{GeV}}{f_a}\right) \left(\frac{\text{GeV}}{T}\right)^4 \quad (3.15)$$

when T is near 1 GeV. The relation between T and t follows as usual from

$$H^2 = \left(\frac{1}{2t}\right)^2 = \frac{8\pi G}{3} \rho = \frac{8\pi G}{3} \cdot \frac{\pi^2}{30} \mathcal{N} T^4 \quad (3.16)$$

where \mathcal{N} is the effective number of thermal degrees of freedom. \mathcal{N} is changing near 1 GeV temperature from a value near 60, valid above the quark-hadron phase transition, to a value of order 30 below that transition. Using $\mathcal{N} \simeq 60$, one has

$$m_a(t) \simeq 0.7 \cdot 10^{20} \frac{1}{\text{sec}} \left(\frac{t}{\text{sec}} \right)^2 \left(\frac{10^{12} \text{GeV}}{f_a} \right), \quad (3.17)$$

which implies:

$$t_1 \simeq 2 \cdot 10^{-7} \text{sec} \left(\frac{f_a}{10^{12} \text{GeV}} \right)^{1/3}. \quad (3.18)$$

The corresponding temperature is:

$$T_1 \simeq 1 \text{GeV} \left(\frac{10^{12} \text{GeV}}{f_a} \right)^{1/6}. \quad (3.19)$$

We will make the usual assumption [6] that the changes in the axion mass are adiabatic [i.e. $\frac{1}{m_a(t)} \frac{dm_a}{dt} \ll m_a(t)$] after t_1 and that the axion to entropy ratio is constant from t_1 till the present. Various ways in which this assumption may be violated are discussed in the papers of ref. [21]. We also assume that the axions do not convert to some other light axion-like particles as discussed in ref. [22].

The above discussion neglects the non-linear terms associated with the self-couplings of the axion. In general, such non-linear terms may cause the higher momentum modes to become populated due to spinodal instabilities and parametric resonance. However, in the case of the axion field, such effects are negligible [6,23].

We are now ready to discuss the vacuum realignment contributions to the cosmological axion energy density.

1. Zero momentum mode

This contribution is due to the fact that, at time t_1 , the axion field averaged over distances less than t_1 has in each horizon volume a random value between $-\pi f_a$ and $+\pi f_a$, whereas the CP conserving, and minimum energy density, value is $a = 0$. The average energy density in this “zero momentum mode” at time t_1 is of order:

$$\rho_a^{\text{vac},0}(t_1) \sim \frac{1}{2} m_a^2(t_1) f_a^2. \quad (3.20)$$

The corresponding average axion number density is:

$$n_a^{\text{vac},0}(t_1) = \frac{1}{m_a(t_1)} \rho_a^{\text{vac},0}(t_1) \sim \frac{f_a^2}{2t_1}. \quad (3.21)$$

Since $m_a(t)$ is assumed to change adiabatically after t_1 , the number of axions is conserved after that time. Hence:

$$n_a^{\text{vac},0}(t) \sim \frac{1}{2} \frac{f_a^2}{t_1} \left(\frac{R_1}{R} \right)^3. \quad (3.22)$$

The axions in this population are non-relativistic and contribute m_a each to the energy.

2. Higher momentum modes

This contribution is due to the fact that the axion field has wiggles about its average value inside each horizon volume. The axion number density and spectrum associated with these wiggles is given in Eq. (3.13). Integrating over $\omega > t^{-1}$, we find:

$$n_a^{vac,1}(t) = n_a^{vac,1}(t_1) \left(\frac{R_1}{R}\right)^3 \sim \frac{1}{2} \frac{f_a^2}{t_1} \left(\frac{R_1}{R}\right)^3 \quad (3.23)$$

for the contribution from vacuum realignment associated with higher momentum modes. The bulk of these axions are non-relativistic after time t_1 and hence each axion contributes m_a to the energy. Note that $n_a^{vac,0}(t)$ and $n_a^{vac,1}(t)$ have the same order of magnitude.

B. String decay

The contribution from axions which were produced in the decay of axion strings has been discussed extensively in the literature. We describe it here for the purpose of completeness and clarity. There is still disagreement about the size of this contribution. We will go rapidly over those points which are not controversial, but indicate explicitly those which are.

Axion strings have energy per unit length:

$$\mu \simeq \int_{L^{-1}}^{v_a} dk \frac{\pi v_a^2}{k} = \pi v_a^2 \ln(v_a L) \quad (3.24)$$

where L is an infra-red cutoff. This is the same formula as Eq. (2.3) but with the integral written in wavevector space. In the early universe, when the strings have random directions relative to one another, L is of order the distance between neighboring strings. The strings move relativistically and decay efficiently into axions. As a result there is approximately one long string per horizon at all times after the temperature has dropped below T_* but before the QCD phase transition. By definition, a long string traverses the horizon. By intersecting each other with reconnection, the long strings produce closed string loops of size smaller than the horizon which decay efficiently into axions.

One long axion string per horizon implies the energy density:

$$\rho_{str}(t) \sim \frac{\pi v_a^2}{t^2} \ln(tv_a) . \quad (3.25)$$

We are interested in the *number* density of axions produced in the decay of axion strings because, as we will soon see, these axions become non-relativistic soon after time t_1 and hence contribute each m_a to the energy. The equations governing the number density $n_a^{str}(t)$ of axions produced in the decay of strings are:

$$\frac{d\rho_{str}}{dt} = -2H\rho_{str} - \frac{d\rho_{str \rightarrow a}}{dt} \quad (3.26)$$

$$\frac{dn_a^{str}}{dt} = -3Hn_a^{str} + \frac{1}{\omega(t)} \frac{d\rho_{str \rightarrow a}}{dt} \quad (3.27)$$

where $\omega(t)$ is defined by:

$$\frac{1}{\omega(t)} = \frac{1}{\frac{d\rho_{str \rightarrow a}}{dt}} \int \frac{d\omega}{\omega} \frac{d\rho_{str \rightarrow a}}{dt d\omega}. \quad (3.28)$$

In Eqs. (3.26-3.28), $\frac{d\rho_{str \rightarrow a}}{dt}(t)$ is the rate at which energy density gets converted from strings into axions at time t , whereas $\frac{d\rho_{str \rightarrow a}}{dt d\omega}$ is the spectrum of axions thus emitted. The term $-2H\rho_{str} = +H\rho_{str} - 3H\rho_{str}$ in Eq. (3.26) takes account of the fact that the Hubble expansion both stretches ($+H\rho_{str}$) and dilutes ($-3H\rho_{str}$) long strings. To obtain $n_a^{str}(t)$ from Eqs. (3.25-3.26), we must know what $\omega(t)$ characterizes the spectrum $\frac{d^2\rho_{str \rightarrow a}}{dt d\omega}$ of axions radiated by cosmic axion strings at time t .

The axions that are radiated at time t are emitted by strings which are bent over a distance scale of order t and are relaxing to lower energy configurations. The main source is closed loops of size t . Two views have been put forth concerning the motion and the radiation spectrum of such loops. One view [7,11] is that such a loop oscillates many times, with period of order t , before it has released its excess energy and that the spectrum of radiated axions is concentrated near $\frac{2\pi}{t}$. Let us call this scenario *A*. A second view [8,12] is that the loop releases its excess energy very quickly and that the spectrum of radiated axions $\frac{d\rho_{str \rightarrow a}}{dt d\omega} \sim \frac{1}{\omega}$ with a high energy cutoff of order v_a and a low energy cutoff of order $\frac{2\pi}{t}$. Let us call this scenario *B*. In scenario *A* one has $\omega(t) \sim \frac{2\pi}{t}$ and hence, for $t < t_1$:

$$n_a^{str,A}(t) \sim \frac{v_a^2}{t} \ln(v_a t), \quad (3.29)$$

whereas in *B* one has $\omega(t) \sim \frac{2\pi}{t} \ln(v_a t)$ and hence:

$$n_a^{str,B}(t) \sim \frac{v_a^2}{t}. \quad (3.30)$$

Comparing Eqs. (3.13), (3.29) and (3.30), one sees that in *A* the contribution from string decay to the cosmological axion energy density dominates by a factor $\ln(v_a t) \sim 100$ over the contribution from vacuum realignment, whereas in *B* the two contributions are of the same order of magnitude.

We have carried out computer simulations [12] of the motion and decay of axion strings with the purpose of deciding between the two possibilities. In scenario *A*, the wavevector spectrum $\frac{dE}{dk}$ of the energy stored in the axion field changes from $\frac{\text{constant}}{k}$, characteristic of the string [see Eq. (3.24)], to a spectrum peaked near $k \sim \frac{2\pi}{t}$ after the string loop has decayed into axions. In scenario *B*, $\frac{dE}{dk}$ does not qualitatively change. To distinguish between the two possibilities, we defined the quantity:

$$N_{ax} \equiv \int dk \frac{dE}{dk} \frac{1}{k}, \quad (3.31)$$

and computed it as a function of time while integrating the equations of motion which follow from Lagrangian (2.1) with $\eta = 0$. In scenario *A*, N_{ax} increases as the spectrum softens, whereas in *B*, N_{ax} remains approximately constant. We found in our simulations that N_{ax} decreases by about 20% during the decay of closed string loops. In the simulations, $\ln(v_a L)$ is in the range 4 to 6. If scenario *A* were correct, N_{ax} should have increased by the factor

$\ln(v_a L) - 1 = 3$ to 5 (depending upon the loop size L) during the decay of loops. So our simulations support scenario B . Note that N_{ax} is the quantity that directly measures the string contribution to the axion cosmological energy density. An important caveat is that the simulations are done for values of $\ln(v_a L)$ much smaller than those, of order 60, which characterize axion strings in the early universe.

We will assume henceforth that axion production by cosmic string decay is consistent with possibility B . Hence:

$$n_a^{str}(t) \sim \frac{v_a^2}{t_1} \left(\frac{R_1}{R} \right)^3 . \quad (3.32)$$

It is of the same order of magnitude as the contributions [Eqs. (3.22) and (3.23)] from vacuum realignment.

C. Domain wall decay

During the QCD phase transition, when the axion acquires mass, the axion strings become the boundaries of axion domain walls. Fig. 3 shows a cross-section of a piece of the universe at that time. In 3 dimensions, the domain walls bounded by string may be like pancakes or they may be long surfaces with holes. Which type of configuration dominates matters little to the arguments given below. It does matter that the universe is relatively free of domain walls which are not bounded by strings, i.e. domain walls which close onto themselves like spheres, donuts and so on. We concluded in section II that such domain walls are in fact very rare.

Near 1 GeV temperature, the time-dependent axion mass is given approximately by Eq. (3.17). The wall energy per unit surface is

$$\sigma(t) \simeq 8f_a^2 m_a(t). \quad (3.33)$$

Since the chiral symmetry breaking phase transition has presumably not taken place yet, we do not use the zero-temperature result Eq. (2.6). As illustrated in Fig. 1, the string at the boundary of a wall is embedded into the wall. Hence its infra-red cutoff L , in the sense of Eqs. (2.3) and (3.24), is of order m_a^{-1} and its energy per unit length is therefore

$$\mu \simeq \pi f_a^2 \ln(f_a/m_a) . \quad (3.34)$$

The surface energy E_σ of a typical (size $\sim t_1$) piece of wall bounded by string is $\sigma(t)t_1^2$ whereas the energy in the boundary is $E_\mu \sim \mu t_1$. There is a critical time t_2 when the ratio

$$\frac{E_\sigma(t)}{E_\mu} \sim \frac{8m_a(t)t_1}{\pi \ln(f_a/m_a)} \quad (3.35)$$

is of order one. Using Eqs. (3.17) and (3.18), we (crudely) estimate :

$$t_2 \simeq 10^{-6} \text{sec} \left(\frac{f_a}{10^{12} \text{GeV}} \right)^{1/3} \quad (3.36)$$

$$T_2 \simeq 600\text{MeV} \left(\frac{10^{12}\text{GeV}}{f_a} \right)^{1/6}. \quad (3.37)$$

After t_2 the dynamics of the walls bounded by string is dominated by the energy in the walls whereas before t_2 it is dominated by the energy in the strings. A string attached to a wall is pulled by the wall's tension. For a straight string and flat wall, the acceleration is:

$$a_s(t) = \frac{\sigma(t)}{\mu} \simeq \frac{8m_a(t)}{\pi \ln(f_a/m_a)} \simeq \frac{m_a(t)}{23} \simeq \frac{1}{t_1} \frac{m_a(t)}{m_a(t_2)}. \quad (3.38)$$

Therefore, after t_2 , each string typically accelerates to relativistic speeds, in the direction of the wall to which it is attached, in less than a Hubble time. We argue below that the string will then unzip the wall, and that the energy stored in the wall gets released in the form of barely relativistic axions. However, before doing so, let us describe the competing decay mechanisms which have been discussed.

One mechanism is emission of gravitational waves [9]. A piece of wall bounded by string of size ℓ , assuming for the moment that it is long lived and that its motion is not damped by friction against the surrounding plasma, oscillates with frequency $\omega \sim \ell^{-1}$ and hence emits gravitational waves. The power P may be estimated using the quadrupole formula:

$$P \sim -\frac{d(\sigma\ell^2)}{dt} \sim G(\sigma\ell^4)^2\omega^6 \sim G\sigma^2\ell^2. \quad (3.39)$$

Indeed, emission of gravitational waves by walls bounded by string of size t_1 is dominated by the wall contribution, rather than the string contribution, after time t_2 . Eq. (3.39) implies the lifetime:

$$\tau_{\text{grav}} \sim (G\sigma)^{-1} \simeq 3.10^3\text{sec} \left(\frac{m_a}{10^{-5}\text{eV}} \right), \quad (3.40)$$

independently of size. Note that a piece of wall bounded by string may self-intersect with reconnection producing two walls bounded by string which may again intersect with reconnection, and so on. This fragmentation does not affect the lifetime (3.40) although it shifts the spectrum of gravitational waves to higher frequencies.

Another energy dissipation mechanism is drag caused by the reflection of particles in the primordial plasma. The reflection coefficients between various particles and axion domain walls are discussed in ref. [20]. It was found there that axions which are not highly relativistic have reflection coefficient of order one and that the dominant friction experienced by the oscillating walls is on the fluid of cold axions that were produced by vacuum realignment and string decay. Consider a bent wall of curvature radius of order t_1 . The tension in the wall provides a driving force per unit surface of order σ/t_1 whereas reflection of cold axions produces a damping force per unit surface of order $2m_a\beta^2n_a$ where β is the velocity of the wall. Adding the contributions from vacuum realignment [Eqs. (3.21) and (3.23)] and from string decay [Eq. (3.32)] we have $n_a(t) \sim \frac{2f_a^2}{t_1} \left(\frac{t_1}{t} \right)^{3/2}$. This neglects the contribution $n_a^{dw}(t)$ of axions produced in the decay of the walls themselves but we will see below that $n_a^{dw}(t)$ is of the same order of magnitude as $n_a^{vac}(t)$ and $n_a^{str}(t)$. Comparing the driving force with the damping force, one concludes that β is of order one immediately after t_1 and hence that the rate of energy dissipation by friction is $P \sim -\frac{d(\sigma\ell^2)}{dt} \sim m_a n_a(t)\ell^2$ which implies:

$$-\frac{d \ln \ell}{dt} \sim \frac{1}{t_1} \left(\frac{t_1}{t} \right)^{3/2}. \quad (3.41)$$

Thus energy dissipation by friction is important just after the domain walls appear but this mechanism soon turns off as the universe becomes dilute.

If emission of gravitational radiation and friction on the cold axion fluid were the only important dissipation mechanisms, the conclusion would be that a typical wall, whether or not bounded by string, loses a large fraction of its energy by friction immediately after t_1 and then lives till a time of order τ_{grav} when it decays into gravitons.

However we find it far more likely that the walls bounded by string decay into axions, long before τ_{grav} . If emission of gravitational waves were the dominant dissipation mechanism, a piece of wall bounded by string of size ℓ , assuming for the moment that it does not reduce its size by self-intersections with reconnection, would oscillate on the order of $\frac{\tau_{grav}}{\ell} \sim 10^{10} \left(\frac{t_1}{\ell} \right) \left(\frac{m_a}{10^{-5} \text{eV}} \right)^{4/3}$ times before decaying away. This seems an implausibly large number considering that nothing forbids the wall from decaying into axions instead. It is especially implausible when one considers that at each oscillation a wall bounded by string may self-intersect with reconnection producing two smaller walls bounded by string. If the two pieces produced by an intersection with reconnection are typically of roughly equal size it takes only $\log_2(m_a t_1) \sim 10$ iterations of this process for the size of the pieces to go down from t_1 to the thickness m_a^{-1} of the walls. Pieces of size m_a^{-1} surely decay into axions because their dynamics is dominated by the energy of the strings and strings are known to decay into axions efficiently. Even if the two pieces produced by a self-intersection with reconnection are typically of very different size, it takes at most $t_1 m_a$ iterations for the pieces to go down in size to m_a^{-1} . Hence for emission of gravitational waves to be the dominant decay mechanism, the probability p of self-intersection with reconnection per oscillation can not be larger than $\frac{t_1^2 m_a}{\tau_{grav}} \simeq 10^{-7} \left(\frac{10^{-5} \text{eV}}{m_a} \right)^{2/3}$. p may reasonably be thought to be of order one. It seems implausible that p could be as small as 10^{-7} .

In section IV we describe our computer simulations of the motion and decay of walls bounded by string. In the simulations the walls decay immediately, i.e. in a time of order their size divided by the speed of light. The average energy of the radiated axions is $\langle \omega_a \rangle \sim 7 m_a$ in the simulations. However, as was already mentioned in the Introduction, the simulations are done for $\ln(v_a/m_a) \simeq \ln(100) \simeq 4.6$, whereas in axion models of interest $\ln(v_a/m_a) \simeq 60$. One reason this may affect the results is the following. When massless the axion field is equivalent, by a duality transformation, to an anti-symmetric two index gauge field $A_{\mu\nu}$ [24]. The axion string is a source for this field. If the string accelerates with acceleration a_s it emits radiation of frequency of order a_s . Since $a_s \simeq \frac{m_a}{23}$ in axion models of interest [see Eq. (3.38)], the emission of axion radiation is inhibited by the fact that a_s is considerably less than m_a , the lowest possible frequency for axion radiation. In the simulations $a_s \simeq 0.6 m_a$.

At any rate, for the reasons given earlier, it is most plausible that the walls bounded by string decay into barely relativistic axions long before τ_{grav} . Let t_3 be the time when the decay effectively takes place and let $\gamma \equiv \frac{\langle \omega_a \rangle}{m_a(t_3)}$ be the average Lorentz γ factor then of the axions produced. In section II, we estimated the density of walls at time t_1 to be of order 0.7 per horizon volume. Hence we estimate that between t_1 and t_3 the average energy density in walls is

$$\rho_{\text{d.w.}}(t) \sim (0.7)(9)m_a(t)\frac{f_a^2}{t_1}\left(\frac{R_1}{R}\right)^3. \quad (3.42)$$

We used Eq. (2.6) and assumed that the energy in walls simply scales as $m_a(t)$. After time t_3 , the number density of axions produced in the decay of walls bounded by strings is of order

$$n_a^{\text{d.w.}}(t) \sim \frac{\rho_{\text{d.w.}}(t_3)}{\langle\omega_a\rangle}\left(\frac{R_3}{R}\right)^3 \sim \frac{6}{\gamma} \frac{f_a^2}{t_1}\left(\frac{R_1}{R}\right)^3. \quad (3.43)$$

Note that the dependence on t_3 drops out of our estimate of $n_a^{\text{d.w.}}$. If we use the value $\gamma = 7$ observed in our computer simulations, we have

$$n_a^{\text{d.w.}}(t) \sim \frac{f_a^2}{t_1}\left(\frac{R_1}{R}\right)^3. \quad (3.44)$$

In that case the contributions from vacuum realignment [Eq. (3.22) and Eq. (3.23)] and domain wall decay are of the same order of magnitude. However, we will find in section IV that γ rises approximately linearly with $\ln(\sqrt{\lambda}v_a/m_a)$ over the range of $\ln(\sqrt{\lambda}v_a/m_a)$ investigated in our numerical simulations. If this behaviour is extrapolated all the way to $\ln(\sqrt{\lambda}v_a/m_a) \simeq 60$, which is the value in axion models of interest, then $\gamma \simeq 60$. In that case the contribution from wall decay is subdominant relative to that from vacuum realignment.

D. The cold axion cosmological energy density

Adding the three contributions, and assuming scenario B for the string contribution, we estimate the present cosmological energy density in cold axions to be:

$$\rho_a(t_0) \sim 3\frac{f_a^2}{t_1}\left(\frac{R_1}{R_0}\right)^3 m_a. \quad (3.45)$$

Following [6], we may determine the ratio of scale factors R_1/R_0 by assuming the conservation of entropy from time t_1 till the present. The number of effective thermal degrees of freedom at time t_1 is approximately $\mathcal{N}_1 \simeq 61.75$. We do not include axions in this number because they are decoupled by then. Let t_4 be a time (say $T_4 = 4$ MeV) after the pions and muons annihilated but before neutrinos decoupled. The number of effective thermal degrees of freedom at time t_4 is $\mathcal{N}_4 = 10.75$ with electrons, photons and three species of neutrinos contributing. Conservation of entropy implies $\mathcal{N}_1 T_1^3 R_1^3 = \mathcal{N}_4 T_4^3 R_4^3$. The neutrinos decouple before e^+e^- annihilation. Therefore, as is well known, the present temperature $T_{\gamma 0} = 2.735$ K of the cosmic microwave background is related to T_4 by: $\frac{11}{2} T_4^3 R_4^3 = 2 T_{\gamma 0}^3 R_0^3$. Putting everything together we have

$$\left(\frac{R_1}{R_0}\right)^3 \simeq 0.063 \left(\frac{T_{\gamma,0}}{T_1}\right)^3. \quad (3.46)$$

Combining Eqs. (3.18), (3.45) and (3.46),

$$\rho_a(t_0) \sim 10^{-29} \frac{\text{gr}}{\text{cm}^3} \left(\frac{f_a}{10^{12}\text{GeV}}\right)^{7/6}. \quad (3.47)$$

Dividing by the critical density $\rho_c = \frac{3H_0^2}{8\pi G}$, we find :

$$\Omega_a \sim \left(\frac{f_a}{10^{12}\text{GeV}} \right)^{7/6} \left(\frac{0.7}{h} \right)^2 \quad (3.48)$$

where h is defined as usual by $H_0 = h \text{ 100km/s}\cdot\text{Mpc}$.

E. Pop. I and Pop. II axions

On the basis of the discussion in section IIIA-D we distinguish two kinds of cold axions:

I) axions which were produced by vacuum realignment or string decay and which were not hit by moving domain walls. They have typical momentum $\langle p_I(t_1) \rangle \sim \frac{1}{t_1}$ at time t_1 because they are associated with axion field configurations which are inhomogeneous on the horizon scale at that time. Their velocity dispersion is of order:

$$\beta_I(t) \sim \frac{1}{m_a t_1} \left(\frac{R_1}{R} \right) \simeq 3 \cdot 10^{-17} \left(\frac{10^{-5}\text{eV}}{m_a} \right)^{5/6} \frac{R_0}{R}. \quad (3.49)$$

Let us call these axions population I.

II) axions which were produced in the decay of domain walls. They have typical momentum $\langle p_{II}(t_3) \rangle \sim \gamma m_a(t_3)$ at time t_3 when the walls effectively decay. Their velocity dispersion is of order:

$$\beta_{II}(t) \sim \gamma \frac{m_a(t_3) R_3}{m_a R} \simeq 10^{-13} \left(\gamma \frac{m_a(t_3) R_3}{m_a R_1} \right) \left(\frac{10^{-5}\text{eV}}{m_a} \right)^{1/6} \frac{R_0}{R}. \quad (3.50)$$

The factor $q \equiv \gamma \frac{m_a(t_3) R_3}{m_a R_1}$ parameterizes our ignorance of the wall decay process. We expect q to be of order one but with very large uncertainties. Fortunately there is a lower bound on q which follows from the fact that the time t_3 when the walls effectively decay must be after t_2 when the energy density in walls starts to exceed the energy density in strings. Using Eq. (3.36), we find:

$$q = \frac{\gamma m_a(t_3) R_3}{m_a R_1} > \frac{\gamma m_a(t_2) R_2}{m_a R_1} \simeq \frac{\gamma}{130} \left(\frac{10^{-5}\text{eV}}{m_a} \right)^{2/3}. \quad (3.51)$$

Since our computer simulations suggest γ is in the range 7 to 60, the axions of the second population (pop. II) have much larger velocity dispersion than the pop. I axions.

Note that there are axions which were produced by vacuum realignment or string decay but were hit by relativistically moving walls at some time between t_1 and t_3 . These axions are relativistic just after getting hit and therefore are part of pop. II rather than pop. I.

The fact that there are two populations of cold axions, with widely differing velocity dispersion, has interesting implications for the formation and evolution of axion miniclusters. This is discussed in section V.

Here we speculate that the primordial velocity dispersion of pop. II axions may some day be measured in a cavity-type axion dark matter detector [18]. If a signal is found in such a detector, the energy spectrum of dark matter axions will be measured with great resolution. It has been pointed out that there are peaks in the spectrum [19] because late infall produces distinct flows, each with a characteristic local velocity vector. These peaks are broadened by the primordial velocity dispersion, given in Eqs. (3.49) and (3.50) for pop. I and pop. II axions respectively. These equations give the velocity dispersion in intergalactic space. When the axions fall onto the galaxy their density increases by a factor of order 10^3 and hence, by Liouville's theorem, their velocity dispersion increases by a factor of order 10. [Note that this increase is not isotropic in velocity space. Typically the velocity dispersion is reduced in the direction longitudinal to the flow in the rest frame of the galaxy whereas it is increased in the two transverse directions.] The energy dispersion measured on Earth is $\Delta E = m_a \beta \Delta \beta$ where $\beta \simeq 10^{-3}$ is the flow velocity in the rest frame of the Earth. Hence we find $\Delta E_I \sim 3 \cdot 10^{-19} \left(\frac{10^{-5} \text{eV}}{m_a}\right)^{5/6} m_a$ for pop. I axions and $\Delta E_{II} \sim 10^{-15} q \left(\frac{10^{-5} \text{eV}}{m_a}\right)^{1/6} m_a$ for pop. II. The minimum time required to measure ΔE is $(\Delta E)^{-1}$. This assumes ideal measurements and also that all sources of jitter in the signal not due to primordial velocity dispersion can be understood. There is little hope of measuring the primordial velocity dispersion of pop. I axions since $(\Delta E_I)^{-1} \sim 10 \text{ years} \left(\frac{10^{-5} \text{eV}}{m_a}\right)^{1/6}$. However $(\Delta E_{II})^{-1} \sim \text{day} q^{-1} \left(\frac{10^{-5} \text{eV}}{m_a}\right)^{5/6}$, and hence it is conceivable that the primordial velocity dispersion of pop. II axions will be measured.

IV. COMPUTER SIMULATIONS

We have carried out an extensive program of 2D numerical simulations of domain walls bounded by strings. The Lagrangian (2.1) in finite difference form is

$$\begin{aligned}
L = \sum_{\vec{n}} \left\{ \frac{1}{2} \left[\left(\dot{\phi}_1(\vec{n}, t) \right)^2 + \left(\dot{\phi}_2(\vec{n}, t) \right)^2 \right] - \sum_{j=1}^2 \frac{1}{2} \left[\left(\phi_1(\vec{n} + \hat{j}, t) - \phi_1(\vec{n}, t) \right)^2 \right. \right. \\
+ \left. \left(\phi_2(\vec{n} + \hat{j}, t) - \phi_2(\vec{n}, t) \right)^2 \right] - \frac{1}{4} \lambda \left[\left(\phi_1(\vec{n}, t) \right)^2 + \left(\phi_2(\vec{n}, t) \right)^2 - 1 \right]^2 \right. \\
\left. + \eta \left(\phi_1(\vec{n}, t) - 1 \right) \right\} \quad (4.1)
\end{aligned}$$

where \vec{n} labels the sites. In these units, $v_a = 1$, the wall thickness is $1/m_a = 1/\sqrt{\eta}$ and the core size is $\delta = 1/\sqrt{\lambda}$. The lattice constant is the unit of length. In the continuum limit, the dynamics depends upon a single critical parameter, namely $m_a \delta = m_a/\sqrt{\lambda}$.

Large two-dimensional grids ($\sim 4000 \times 4000$) were initialized with a straight or curved domain wall, at rest or with angular momentum. The initial domain wall was obtained by overrelaxation, starting with the Sine-Gordon ansatz $\phi_1 + i\phi_2 = \exp(4i \tan^{-1} \exp(m_a y))$ inside a strip of length the distance D between the string and anti-string, and the true vacuum ($\phi_1 = 1, \phi_2 = 0$) outside. The string and anti-string cores were approximated by $\phi_1 + i\phi_2 = -\tanh(.583 r/\delta) \exp(\mp i\theta)$, where r and θ are polar coordinates about the core center, and held fixed during relaxation. Stable domain walls were obtained for $1/(m_a \delta) \gtrsim 3$. A first-order in time and second-order in space algorithm was used for the dynamical

evolution, with time step $dt = 0.2$. The boundary conditions were periodic throughout and the total energy was conserved to better than 1%. If the angular momentum was nonzero, the initial $\dot{\phi}$ was obtained as the difference of two relaxed wall configurations a small time step apart, divided by that time step.

The evolution of the domain wall was studied for various values of $\sqrt{\lambda}/m_a$, the initial wall length D and the initial velocity v of the strings in the direction transverse to the wall, the string and anti-string going in opposite directions. The strings attached to the wall are rapidly accelerated by the wall tension, the potential and gradient energies of the wall being converted into kinetic energy of the strings. Fig. 4 shows the longitudinal velocity of the core as a function of time for the case $m_a^{-1} = 400$, $\sqrt{\lambda}/m_a = 10$ and $v = 0$. An important feature is the Lorentz contraction of the core. For reduced core sizes $\delta/\gamma_s \lesssim 5$, where γ_s is the Lorentz factor associated with the speed of the string core, there is ‘scraping’ of the core on the lattice accompanied by emission of spurious high frequency radiation. This artificial friction eventually balances the wall tension and leads to a terminal velocity. In our simulations we always ensured being in the continuum limit.

For a domain wall without rotation ($v = 0$), the string cores meet head-on and go through each other. Several oscillations of decreasing magnitude generally occur before annihilation. For $\gamma_s \simeq 1$ the string and anti-string coalesce and annihilate one another. For $\gamma_s \gtrsim 2$, the strings go through each other and regenerate a new wall of reduced length. The relative oscillation amplitude decreases with decreasing collision velocity. Fig. 5 shows the core position as a function of time for the case $m_a^{-1} = 1000$, $\sqrt{\lambda}/m_a = 14.3$, $D = 2896$. Fig. 6a shows the gradient, kinetic, string potential, wall potential and total energies as a function of time. By ‘string (wall) potential’ energy, we mean the energy associated with the third (fourth) term in Eq. (4.1). The total energy is accurately conserved in spite of the violent goings-on when the string and anti-string meet.

We also investigated the more generic case of a domain wall with angular momentum. The strings are similarly accelerated by the wall but string and anti-string cores rotate around each other. Fig. 6b shows the gradient, kinetic, string potential, wall potential and total energies as a function of time for the case $m_a^{-1} = 500$, $\sqrt{\lambda}/m_a = 28.3$, $D = 2096$, and $v = 0.25$. The field is displayed in Fig. 7 at various time steps for the case $m_a^{-1} = 100$, $\lambda = 0.01$, $D = 524$ and $v = 0.6$. No oscillation is observed. All energy is converted into axion radiation during a single collapse. Oscillations occur only when the angular momentum is too small for the string and anti-string cores to miss each other.

We performed spectrum analysis of the energy stored in the ϕ field as a function of time using standard Fourier techniques. The two-dimensional Fourier transform is defined by

$$\tilde{f}(\vec{p}) = \frac{1}{\sqrt{L_x L_y}} \sum_{\vec{n}} \exp \left[2i\pi \left(\frac{p_x n_x}{L_x} + \frac{p_y n_y}{L_y} \right) \right] f(\vec{n}) \quad (4.2)$$

for $p_j = 1, \dots, L_j$ where $j = x, y$. The dispersion law is:

$$\omega_p = \sqrt{2 \left(2 - \cos \frac{2\pi p_x}{L_x} - \cos \frac{2\pi p_y}{L_y} \right) + m_a^2}. \quad (4.3)$$

Fig. 8 shows the power spectrum $dE/d \log \omega$ of the ϕ field at various times during the decay of a rotating domain wall for the case $m_a^{-1} = 500$, $\lambda = 0.0032$, $D = 2096$, and $v = 0.25$.

Initially, the spectrum is dominated by small wavevectors, $k \sim m_a$. Such a spectrum is characteristic of the domain wall. As the wall accelerates the string, the spectrum hardens until it becomes roughly $1/k$ with a long wavelength cutoff of order the wall thickness $1/m_a$ and a short wavelength cutoff of order the reduced core size δ/γ_s . Such a spectrum is characteristic of the moving string. In the case of the figure, the string and anti-string cores annihilate at about the time of the fourth frame (Fig. 8d). The spectrum remains approximately $1/k$ during the annihilation process and thereafter.

As discussed in section IIIC, $\gamma = \langle \omega_a \rangle / m_a$, the average energy of the radiated axions in units of the axion mass, is the quantity which determines the wall decay contribution to the axion cosmological energy density [see Eq. (3.43)]. Fig. 9 shows the time evolution of $\langle \omega \rangle / m_a$ for $m_a^{-1} = 500$, $v = 0.25$, $D = 2096$ and various values of λ . By definition,

$$\langle \omega \rangle = \sum_{\vec{p}} E_{\vec{p}} / \sum_{\vec{p}} \frac{E_{\vec{p}}}{\omega_{\vec{p}}} \quad (4.4)$$

where $E_{\vec{p}}$ is the gradient and kinetic energy stored in mode \vec{p} of the field ϕ . After the domain wall has decayed into axions, $\langle \omega \rangle = \langle \omega_a \rangle$. Fig. 10 shows the time evolution of $\langle \omega \rangle / m_a$ for $m_a^{-1} = 500$, $\lambda = 0.0016$, $D = 2096$ and various values of v . For small v and/or small λ , i.e. when the angular momentum is low and the core size is big, the string cores meet head on and the strings have one or more oscillations. In that case, $\langle \omega_a \rangle / m_a \simeq 4$. This is consistent with the value, $\langle \omega_a \rangle / m_a \simeq 3$, found by Nagasawa and Kawasaki [14]. The low angular momentum regime, when the strings oscillate, is characterized by low energy of the radiated axions. We believe this regime to be less relevant to wall decay in the early universe because it seem unlikely that the angular momentum of a wall at the QCD epoch could be small enough for the strings to oscillate then, especially when one considers that the actual wall configurations are 3 dimensional rather than 2D.

In the more generic case when no oscillations occur, $\langle \omega_a \rangle / m_a \simeq 7$. Moreover, we find that $\langle \omega_a \rangle / m_a$ depends upon the critical parameter $\sqrt{\lambda}/m_a$, increasing approximately as the logarithm of that quantity; see Fig. 9. This is consistent with the time evolution of the energy spectrum, described in Fig. 8. For a domain wall, $\langle \omega \rangle \sim m_a$ whereas for a moving string $\langle \omega \rangle \sim m_a \ln(\sqrt{\lambda} v_a \gamma_s / m_a)$. Since we find the decay to proceed in two steps: 1) the wall energy is converted into string kinetic energy, and 2) the strings annihilate without qualitative change in the spectrum, the average energy of radiated axions is $\langle \omega_a \rangle \sim m_a \ln(\sqrt{\lambda} v_a / m_a)$. Assuming this is a correct description of the decay process for $\sqrt{\lambda} v_a / m_a \sim 10^{26}$, then $\langle \omega_a \rangle / m_a \sim 60$ in axion models of interest.

Present technology is inadequate for 3D simulations with sufficient resolution for the purposes we are interested in, such as obtaining reliable estimates of the factor γ . However, lower resolution 3D and 2D simulations of string-wall networks were carried out in ref. [26]. They showed qualitatively similar behaviour in 2 and 3 dimensions.

V. AXION MINICLUSTERS

We saw in section III that the axion fluid is inhomogeneous with $\frac{\delta \rho_a}{\rho_a} = \mathcal{O}(1)$ at the time of the QCD phase transition. As will be discussed below, the streaming length of the pop. I axions (those from vacuum realignment and string decay) is too short for all these

inhomogeneities to get erased by free streaming before the time t_{eq} of equality between matter and radiation. t_{eq} is when density perturbations start to grow by gravitational instability. At time t_{eq} , the $\frac{\delta\rho_a}{\rho_a} = \mathcal{O}(1)$ inhomogeneities in the axion fluid promptly form gravitationally bound objects, called axion miniclusters [16,17]. Of course, axion miniclusters occur only if there is no inflation or if inflation occurs with reheat temperature above the phase transition where $U_{PQ}(1)$ is spontaneously broken.

Axion miniclusters were discussed in the seminal papers of Hogan and Rees [16], and of Kolb and Tkachev [17]. However, in these pioneering studies the role of domain walls, and hence of axions from domain wall decay, was neglected. Also the estimates of the minicluster mass have varied considerably from one another. Hence we think it appropriate to give our own analysis of this interesting phenomenon.

As described in section III, there are two populations of cold axions, pop. I and pop. II, with velocity dispersions given by Eqs.(3.49) and (3.50) respectively. Both populations are inhomogeneous with $\frac{\delta\rho_a}{\rho_a} = \mathcal{O}(1)$ at the time of the QCD phase transition. The free streaming length from time t_1 to t_{eq} is:

$$\ell_f = R(t_{eq}) \int_{t_1}^{t_{eq}} dt \frac{\beta(t)}{R(t)} \simeq \beta(t_1) \sqrt{t_1 t_{eq}} \ln \left(\frac{t_{eq}}{t_1} \right). \quad (5.1)$$

For the sake of definiteness, we assume henceforth $\Omega_0 = 1$ and $H_0 = 60$ km/s.Mpc, in which case $T_{eq} = 2$ eV. The free streaming length should be compared with the size

$$\ell_{mc} \sim t_1 \frac{R_{eq}}{R_1} \simeq \sqrt{t_1 t_{eq}} \simeq 0.7 \cdot 10^{13} \text{cm} \left(\frac{10^{-5} \text{eV}}{m_a} \right)^{1/6} \quad (5.2)$$

of axion inhomogeneities at time t_{eq} . Using Eq.(3.49) we find for pop. I:

$$\frac{\ell_{f,I}}{\ell_{mc}} \simeq \frac{1}{t_1 m_a} \ln \left(\frac{t_{eq}}{t_1} \right) \simeq 1.6 \cdot 10^{-2} \left(\frac{10^{-5} \text{eV}}{m_a} \right)^{2/3}. \quad (5.3)$$

Hence, in the axion mass range of interest, pop. I axions do not homogenize. At t_{eq} many pop. I axions condense into miniclusters since they have $\frac{\delta\rho}{\rho} = \mathcal{O}(1)$ upon arrival. The typical size of axion miniclusters is ℓ_{mc} and their typical mass is:

$$M_{mc} \sim \frac{1}{4} \rho_a(t_{eq}) \frac{4\pi}{3} \left(\frac{\ell_{mc}}{2} \right)^3 \sim 0.7 \cdot 10^{-13} M_\odot \left(\frac{10^{-5} \text{eV}}{m_a} \right)^{5/3}. \quad (5.4)$$

We assumed that half the cold axions are pop. I and that half of those form miniclusters, hence the factor 1/4. We used Eq. (3.48) to estimate $\rho_a(t_{eq})$.

Using Eq. (3.50), we find for pop. II:

$$\frac{\ell_{f,II}}{\ell_{mc}} \sim q \ln \left(\frac{t_{eq}}{t_3} \right) \simeq 40 q. \quad (5.5)$$

Using Eq. (3.51) and the range $\gamma \sim 7$ to 60, suggested by our numerical simulations, we conclude that pop. II axions do homogenize and hence that the axion energy density has a smooth component at t_{eq} .

At time t , pop. II axions get gravitationally bound to the nearest minicluster if it is less than distance $d \sim GM_{mc}/\beta_{II}(t)^2$ away. Since most are at a distance $d(t) \sim \ell_{mc} \frac{T_{eq}}{T(t)}$, the bulk of pop. II axions become gravitationally bound to miniclusters when the temperature has dropped to:

$$T_{II} \sim 4 \cdot 10^{-3} \frac{T_{eq}}{q^2}, \quad (5.6)$$

assuming $\Omega_a \sim 1$. Thus we arrive at a qualitative picture of miniclusters before galaxy formation as having an inner core of pop. I axions and a fluffy outer envelope of pop. II axions. The inner core has size ℓ_{mc} and density

$$\rho_{mc} \sim 10^{-18} \frac{\text{gr}}{\text{cm}^3}. \quad (5.7)$$

If $T_{II} > T_0$ (i.e. $q \lesssim 6$), the outer envelope has roughly the same mass as the core but size

$$\ell'_{mc} \sim 2 q^2 10^{15} \text{cm} \quad (5.8)$$

and density

$$\rho'_{mc} \sim q^{-6} 10^{-25} \frac{\text{gr}}{\text{cm}^3}. \quad (5.9)$$

If $T_{II} < T_0$, then the envelope is correspondingly less massive and less dense. When a minicluster falls onto a galaxy, tidal forces of the galaxy are apt to destroy it. We find below that the outer envelopes almost surely get pulled off whereas the inner cores barely survive.

When a minicluster passes by an object of mass M with impact parameter b and velocity v , the internal energy per unit mass ΔE given to the minicluster by the tidal gravitational forces from that object is of order [16]

$$\Delta E \sim \frac{G^2 M^2 \ell_{mc}^2}{b^4 \beta^2} \quad (5.10)$$

whereas the binding energy per unit mass of the minicluster $E \sim G \rho_{mc} \ell_{mc}^2$. If the minicluster travels a length $\ell = \beta t$ through a region where objects of mass M have density n , the relative increase in internal energy is:

$$\frac{\Delta E}{E} \sim \frac{G \rho_M^2 t^2}{\rho_{mc}}, \quad (5.11)$$

where $\rho_M = Mn$. Eq. (5.11) follows from the fact that ΔE is dominated by the closest encounter and the latter has impact parameter $b_{min}: \pi b_{min}^2 n \ell = 0(1)$. Note that $\frac{\Delta E}{E}$ is independent of M . The effect upon a minicluster of falling once with velocity $\beta \simeq 10^{-3}$ through the inner halo ($r < 10$ kpc) of our galaxy where $\rho_M \sim 10^{-24} \text{gr}/\text{cm}^3$ is:

$$\begin{aligned} \frac{\Delta E}{E} \sim \frac{\rho_M}{\rho_{mc}} &\sim 10^{-6} && \text{for the inner core} \\ &\sim 10 q^6 && \text{for the outer envelope} \end{aligned} \quad (5.12)$$

Since we expect q to be of order one, it seems very likely that the envelope gets pulled off after one or more crossings of the inner parts of the galaxy. This result is reassuring for direct searches of dark matter axions on Earth since it implies that a smooth component of dark matter axions with density of order ρ_{halo} permeates us whether or not there is inflation after the Peccei-Quinn phase transition. If there were no pop. II axions one might fear that nearly all axions are in axion miniclusters.

This result can also be obtained by considering the tidal radius of a mini-cluster at our location in the galaxy:

$$R_{tidal} \sim \left(\frac{M_{mc}}{3M_{gal}}\right)^{1/3} D \sim 8 \cdot 10^{13} \text{cm} \left(\frac{10^{-5} \text{eV}}{m_a}\right)^{5/9} \quad (5.13)$$

where $D \simeq 8.5$ kpc is our distance from the galactic center and $M_{gal} \simeq 10^{12} M_{\odot}$ is the mass of the galaxy interior to us. R_{tidal} is larger than the inner core size ℓ_{mc} but smaller than the outer envelope ℓ'_{mc} .

A minicluster inner core which has spent most of its life in the central part of our galaxy only barely survived since $\frac{\Delta E}{E} \sim 10^{-2}$ in that case. If most minicluster inner cores have survived more or less intact, the direct encounter of a minicluster with Earth would still be quite rare, happening only every 10^4 years or so. The encounter would last for about 3 days during which the local axion density would increase by a factor of order 10^6 .

VI. THE THIRD SOLUTION TO THE AXION DOMAIN WALL PROBLEM

In this section we consider axion models in which the number N of degenerate vacua at the bottom of the Mexican hat potential is larger than one. N is an integer given by

$$\text{Tr}(Q_{PQ} Q_c^a Q_c^b) = N \delta^{ab}. \quad (6.1)$$

Here Q_{PQ} is the Peccei-Quinn charge, Q_c^a ($a = 1 \dots 8$) are the color charges and Tr represents a sum over all the left-handed Weyl spinors in the model. It is easy to construct models for an arbitrary value of N .

There are N distinct degenerate equally spaced vacua at the bottom of the Mexican hat potential [3]. The vacua are related by an exact spontaneously broken $Z(N)$ symmetry. A domain wall is a transition in space from any one vacuum to a distinct neighboring vacuum. A string is the boundary of N walls. If $N > 1$ and there is no inflation after the Peccei-Quinn phase transition, axion models suffer from a domain wall problem because the energy density in walls ends up exceeding the energy density in matter and radiation. A domain wall dominated universe is very much unlike our own. The walls are gravitationally repulsive [25]. The universe is divided into rapidly expanding bubbles with walls at the boundaries and islands of matter in the middles. When averaged on scales larger than the bubble size, the universe expands as $R \sim t^2$ [27]. At least in the case of axion walls, the islands are far too small for one island to be identified with our visible universe.

The axion domain wall problem can be solved 1) by having inflation with reheating temperature less than the PQ phase transition temperature, or 2) by having $N = 1$ as discussed in the other sections of this paper, or 3) by having a small explicit breaking of the $Z(N)$ symmetry [3]. The third solution is discussed in this section. The symmetry breaking

must lift completely the degeneracy of the vacuum and be large enough that the unique true vacuum takes over before the walls dominate the energy density. On the other hand, it must be small enough that the PQ mechanism still works. The implications of biased discrete symmetry breaking have been discussed in a general manner in ref. [28].

We may, for our purposes, take the effective action density for the axion field to be:

$$\mathcal{L}_a = \frac{1}{2} \partial_\mu a \partial^\mu a + \frac{m_a^2 v_a^2}{N^2} \left[\cos \left(\frac{Na}{v_a} \right) - 1 \right]. \quad (6.2)$$

The axion field $a(x)$ is cyclic with period $2\pi v_a$. Thus Eq. (6.2) implies N degenerate vacua. The axion decay constant is $f_a \equiv \frac{v_a}{N}$. The domain wall is a transition in space from a vacuum, say $a = 0$, to a neighbor vacuum, say $a = \frac{2\pi v_a}{N}$. The energy per unit surface is $\sigma = 8m_a f_a^2$. The actual axion domain wall is only crudely described by Eq. (6.2) because it involves not only a rotation of the axion field but also of the quark-antiquark condensates. However Eq. (6.2) is adequate for the order of magnitude estimates we are interested in here.

Between the PQ and QCD phase transitions, axion strings are present and evolve as in the $N = 1$ case. At time t_1 each string becomes the boundary of N walls. For a brief period the walls lose energy by friction against the primordial plasma but this dissipation process is soon turned off as the plasma becomes dilute.

Causality implies that there is at least one domain wall per horizon on average since each horizon volume picks a vacuum independently from its neighbor. If there is of order one wall per horizon, the energy density in walls $\rho \sim \frac{\sigma t^2}{t^3} = \frac{\sigma}{t}$. In that case, the energy in walls per co-moving volume ($E \sim \rho R^3 \sim \sqrt{t}$) increases with time. This suggests that there is not more than approximately one wall per horizon because energy in walls has low entropy and hence increases only reluctantly.

With one wall per horizon, the fraction of the energy density in walls is

$$\Omega_{d.w.}(t) \sim \frac{32\pi G t \sigma}{3} \sim 2 \cdot 10^{-9} \left(\frac{10^{-5} \text{eV}}{m_a} \right)^{4/3} \frac{t}{t_1}. \quad (6.3)$$

If this fraction reaches one, the universe becomes domain wall dominated and disaster strikes as described above. To get rid of the walls, we add to the model a tiny $Z(N)$ breaking term which lifts the vacuum degeneracy completely, e.g.:

$$\delta V = -\xi(\varphi e^{-i\delta} + h.c.) \quad (6.4)$$

where φ is the PQ field with the ‘‘Mexican hat’’ potential, at the bottom of which $\varphi(x) = v_a e^{ia(x)/v_a}$. On the RHS of Eq.(6.2) an extra term appears:

$$\delta \mathcal{L}_a = 2v_a \xi \cos \left(\frac{a}{v_a} - \delta \right). \quad (6.5)$$

Now the unique true vacuum is the one for which $|\delta - \frac{a}{v_a}|$ is smallest. Its energy density is lowered by an amount of order ξv_a relative to the other quasi-vacua. As a result, the walls at the boundary of a region in the true vacuum are subjected to an outward pressure of order ξv_a . Since the walls are typically a distance t apart, the volume energy $\xi v_a t^3$ associated with the lifting of the vacuum degeneracy grows more rapidly than the energy σt^2 in the

walls. At a time $\tau \sim \frac{\sigma}{\xi v_a}$, the pressure favoring the true vacuum starts to dominate the wall dynamics and the true vacuum takes over, i.e. the walls disappear. We require this to happen before the walls dominate the energy density. Using Eqs. (3.18) and (6.3), we obtain:

$$\tau \sim \frac{\sigma}{\xi v_a} \lesssim 10^2 \text{ sec} \left(\frac{m_a}{10^{-5} \text{eV}} \right). \quad (6.6)$$

On the other hand ξ is bounded from above by the requirement that δV does not upset the PQ mechanism. δV shifts the minimum of the effective potential for the axion field, inducing a $\bar{\theta} \sim \frac{\xi}{m_a^2 f_a}$. The requirement that $\bar{\theta} < 10^{-10}$ implies:

$$\tau \gtrsim \text{sec} \left(\frac{10^{-5} \text{eV}}{m_a} \right). \quad (6.7)$$

Eqs. (6.6) and (6.7) indicate that there is very little room in parameter space for this third solution to the axion domain wall problem, at least if $m_a \sim 10^{-5}$ eV. But the third solution is not completely ruled out.

Soon after time τ , a cross-section of a small fraction of the universe looks like Fig. 3 except that every string – anti-string pair is connected by N walls instead of just one wall. This likely changes the mechanism by which the walls bounded by strings dissipate their energy since each string is being pulled in different directions by the N walls to which it is attached.

The fraction r of wall energy that goes into non-relativistic or barely relativistic axions is at any rate severely restricted since τ is much earlier than the time $t_{eq} \sim 3 \cdot 10^{11}$ sec of equality between matter and radiation and, using Eqs. (6.3) and (6.7),

$$\Omega_{d.w.}(\tau) \sim 10^{-2} \left(\frac{10^{-5} \text{eV}}{m_a} \right) \frac{\tau}{\text{sec}} \gtrsim 10^{-2} \left(\frac{10^{-5} \text{eV}}{m_a} \right)^2. \quad (6.8)$$

The fraction of the cosmological energy density in axions from domain wall decay

$$\Omega_a^{d.w.}(t) = r \Omega_{d.w.}(\tau) \left(\frac{t}{\tau} \right)^{1/2} \quad (6.9)$$

should be less than about 1/2 when $t = t_{eq}$. This implies the bound

$$r \lesssim 10^{-4} \left(\frac{m_a}{10^{-5} \text{eV}} \right) \left(\frac{\text{sec}}{\tau} \right)^{1/2} \lesssim 10^{-4} \left(\frac{m_a}{10^{-5} \text{eV}} \right)^{3/2}, \quad (6.10)$$

where we used Eq. (6.7) to obtain the second inequality.

However emission of gravitational waves is likely to be very effective because $\tau_{g.w.}$, given by Eq. (3.40), is not very much larger than τ . Thus decay of the walls into gravitational radiation is in this case both necessary and likely. The third solution therefore predicts a peak in the present spectrum of gravitational waves at the frequency

$$\omega_0 \sim \frac{1}{\tau} \left(\frac{R_\tau}{R_0} \right) \sim 2 \cdot 10^{-10} \text{ Hz} \left(\frac{\text{sec}}{\tau} \right)^{1/2}. \quad (6.11)$$

The energy density in these gravitational waves is of order

$$\rho_{g.w.}(t_0) \sim 10^{-2} \rho_\gamma(t_0) \left(\frac{10^{-5} \text{eV}}{m_a} \right) \frac{\tau}{\text{sec}}, \quad (6.12)$$

where $\rho_\gamma(t_0)$ is the energy density in the cosmic microwave background.

VII. CONCLUSIONS.

We have discussed the fate of the walls bounded by strings which appear during the QCD phase transition in axion models with $N = 1$ assuming the axion field is not homogenized by inflation. We have argued that the main decay mechanism of these objects is radiation of barely relativistic axions and that the decay takes place during or soon after the QCD phase transition.

We presented the results of our computer simulations of the motion and decay of walls bounded by strings. In the simulations, the walls decay immediately, i.e. in a time scale of order the light travel time. The computer simulations also provide an estimate of the average energy of the axions emitted in the decay of the walls: $\langle\omega_a\rangle \simeq 7m_a$ when $\sqrt{\lambda}v_a/m_a \simeq 20$.

Because of restrictions on the available lattice sizes, the simulations are for values of v_a/m_a of order 100, whereas in axion models of interest v_a/m_a is of order 10^{26} . To address this shortcoming, we have investigated the dependence of $\langle\omega_a\rangle/m_a$ upon $\sqrt{\lambda}v_a/m_a$ and found that it increases approximately as the logarithm of this quantity. This is because the decay process occurs in two steps: 1) wall energy converts into moving string energy because the wall accelerates the string, and the energy spectrum hardens accordingly; 2) the strings annihilate into axions without qualitative change in the energy spectrum. If this behaviour persists all the way to $\sqrt{\lambda}v_a/m_a \sim 10^{26}$, then $\langle\omega_a\rangle/m_a \sim 60$ for axion models of interest.

To parameterize our ignorance of the decay process we introduced two parameters: the time t_3 when the decay effectively takes place and the average Lorentz factor $\gamma = \langle\omega_a\rangle/m_a$ of the radiated axions at time t_3 . We found that in first approximation the cosmological energy density of axions from wall decay does not depend upon t_3 whereas it is inversely proportional to γ . For $\gamma \sim 7$ the contribution from wall decay is of the same order of magnitude as that from vacuum realignment. All three contributions - vacuum realignment, string decay and wall decay - were discussed in one unified treatment.

We discussed the velocity dispersion of axions from wall decay (pop. II) and found that it is much larger, by a factor 10^3 or so, than that of axions from vacuum realignment and from string decay (pop. I). This has interesting consequences for the formation and evolution of axion miniclusters. We showed that the QCD horizon scale density perturbations in pop.II axions get erased by free streaming before the time t_{eq} of equality between radiation and matter whereas those in pop.I axions do not. Pop. II axions form an unclustered component of the axion cosmological energy density which guarantees that the signal in direct searches for axion dark matter is on all the time.

We speculated that the velocity dispersion of axions from wall decay may be large enough to be measured in a cavity detector of dark matter axions. This would provide a direct experimental handle on some of the issues raised by axion cosmology, e.g. the question whether inflation occurred below or above the PQ phase transition.

Finally we discussed the cosmology of axion models with $N > 1$ in which the axion domain wall problem is solved by postulating a small $U_{PQ}(1)$ breaking interaction which slightly lowers one of the N vacua with respect to the others. There is very little room in parameter space for this to work but it is a logical possibility. We find that in this case the walls must decay into gravitational radiation of frequency of order 10^{-10}Hz .

ACKNOWLEDGMENTS

We thank E.W. Kolb and E.P.S. Shellard for useful comments. PS was the beneficiary of a Fellowship from the J.S. Guggenheim Memorial Foundation. This research was also supported in part by DOE grant DE-FG05-86ER40272 at the University of Florida and by DOE grant W-7405-ENG-048 at Lawrence Livermore National Laboratory.

REFERENCES

- [1] R. D. Peccei and H. Quinn, Phys. Rev. Lett. **38**, 1440 (1977); Phys. Rev. **D16**, 1791 (1977); S. Weinberg, Phys. Rev. Lett. **40**, 223 (1978); F. Wilczek, Phys. Rev. Lett. **40**, 279 (1978).
- [2] J. E. Kim, Phys. Rep. **150**, 1 (1987); H.-Y. Cheng, Phys. Rep. **158**, 1 (1988); R. D. Peccei, in *CP Violation*, Ed. by C. Jarlskog, World Scientific Publ., 1989, pp 503-551; M. S. Turner, Phys. Rep. **197**, 67 (1990); G. G. Raffelt, Phys. Rep. **198**, 1 (1990).
- [3] P. Sikivie, Phys. Rev. Lett. **48**, 1156 (1982).
- [4] H.-T. Janka, W. Keil, G. Raffelt and D. Seckel, Phys. Rev. Lett. **76**, 2621 (1996); W. Keil, H.-T. Janka, D.N. Schramm, G. Sigl, M.S. Turner and J. Ellis, Phys. Rev. **D56**, 2419 (1997).
- [5] D. J. Gross R. D. Pisarski and L. G. Yaffe, Rev. Mod. Phys. **53**, 43 (1981).
- [6] L. Abbot and P. Sikivie, Phys. Lett. **B120**, 133 (1983); J. Preskill, M. Wise and F. Wilczek, Phys. Lett. **B120**, 127 (1983); M. Dine and W. Fischler, Phys. Lett. **120**, 137 (1983).
- [7] R. Davis, Phys. Rev. **D32**, 3172 (1985); Phys. Lett. **B180**, 225 (1986).
- [8] D. Harari and P. Sikivie, Phys. Lett. **B195**, 361 (1987).
- [9] A. Vilenkin and A.E. Everett, Phys. Rev. Lett. **48**, 1867 (1982).
- [10] P. Sikivie in *Where are the elementary particles*, Proc. of the 14th Summer School on Particle Physics, Gif-sur-Yvette, 1982, edited by P. Fayet et al. (Inst. Nat. Phys. Nucl. Phys. Particules, Paris, 1983).
- [11] A. Vilenkin and T. Vachaspati, Phys. Rev. **D35**, 1138 (1987); R.L. Davis and E.P.S. Shellard, Nucl. Phys. **B324**, 167 (1989); A. Dabholkar and J.M. Quashnock, Nucl. Phys. **B333**, 815 (1990); R.A. Battye and E.P.S. Shellard, Nucl. Phys. **B423**, 260 (1994); Phys. Rev. Lett. **73**, 2954 (1994); (E) *ibid.* **76**, 2203 (1996); astro-ph/9802216.
- [12] C. Hagmann and P. Sikivie, Nucl. Phys. **B363**, 247 (1991); C. Hagmann, S. Chang and P. Sikivie, to be published.
- [13] D. H. Lyth, Phys. Lett. **B275**, 279 (1992).
- [14] M. Nagasawa and M. Kawasaki, Phys. Rev. **D50**, 4821 (1994).
- [15] E.W. Kolb and M.S. Turner, *The Early Universe*, Addison-Wesley, 1990.
- [16] C. J. Hogan and M. J. Rees, Phys. Lett. **B205**, 228 (1988).
- [17] E. W. Kolb and I. Tkachev, Phys. Rev. Lett. **71**, 3051 (1993).
- [18] P. Sikivie, Phys. Rev. Lett. **51**, 1415 (1983) and Phys. Rev. **D32**, 2988 (1985); L. Krauss et al., Phys.Rev. Lett. **55**, 1797 (1985); S. DePanfilis et al., Phys. Rev. Lett. **59**, 839 (1987) and Phys. Rev. **D40**, 3151 (1989); C. Hagmann et al., Phys. Rev. **D42**, 1297 (1990); K. van Bibber et al., Int. J. Mod. Phys. **D3** Suppl. 33 (1994); S. Matsuki et al., Phys. Lett. **336**, 573 (1994); C. Hagmann et al, Phys. Rev. Lett. **80**, 2043 (1998).
- [19] P. Sikivie and J. Ipser, Phys. Lett. **B291**, 288 (1992); P. Sikivie, I. Tkachev and Y. Wang, Phys. Rev. Lett. **75**, 2911 (1995) and Phys. Rev. D **56**, 1863 (1997).
- [20] M.C. Huang and P. Sikivie, Phys. Rev. **32**, 1560 (1985).
- [21] P. J. Steinhardt and M. S. Turner, Phys. Lett. **B129**, 51 (1983); W. G. Unruh and R. M. Wald, Phys. Rev. **D32**, 831 (1985); M. S. Turner, Phys. Rev. **D32**, 843 (1985); T. DeGrand, T. W. Kephart and T. J. Weiler, Phys. Rev. **D33**, 910 (1986); G. Lazarides, R. Schaefer, D. Seckel and Q. Shafi, Nucl. Phys. **B346**, 193 (1990); M. Hindmarsh, Phys. Rev. **D45**, 1130 (1992).

- [22] C. T. Hill and G. G. Ross, Nucl. Phys. **B311**, 253 (1988).
- [23] E.W. Kolb, A. Singh and M. Srednicki, hep-ph/9709285; P.B. Greene, L. Kofman and A.A. Starobinsky, hep-ph/9808477.
- [24] M. Kalb and P. Ramond, Phys. Rev. **D9**, 2273 (1974); F. Lund and T. Regge, Phys. Rev. **D14**, 1524 (1976); E. Witten, Phys. Lett. **B153**, 243 (1985).
- [25] A. Vilenkin, Phys. Lett. **B133**, 177 (1983); J. Ipser and P. Sikivie, Phys. Rev. **D30**, 712 (1984).
- [26] B.S. Ryden, W.H. Press and D.N. Spergel, Ap. J. **357**, 293 (1990).
- [27] Y. Zel'dovich, Y. Kobzarev and L. Okun, Sov. Phys. JETP **40**,1 (1975).
- [28] G.B. Gelmini, M. Gleiser and E.W. Kolb, Phys. Rev. **D39**, 1558 (1989).

FIGURES

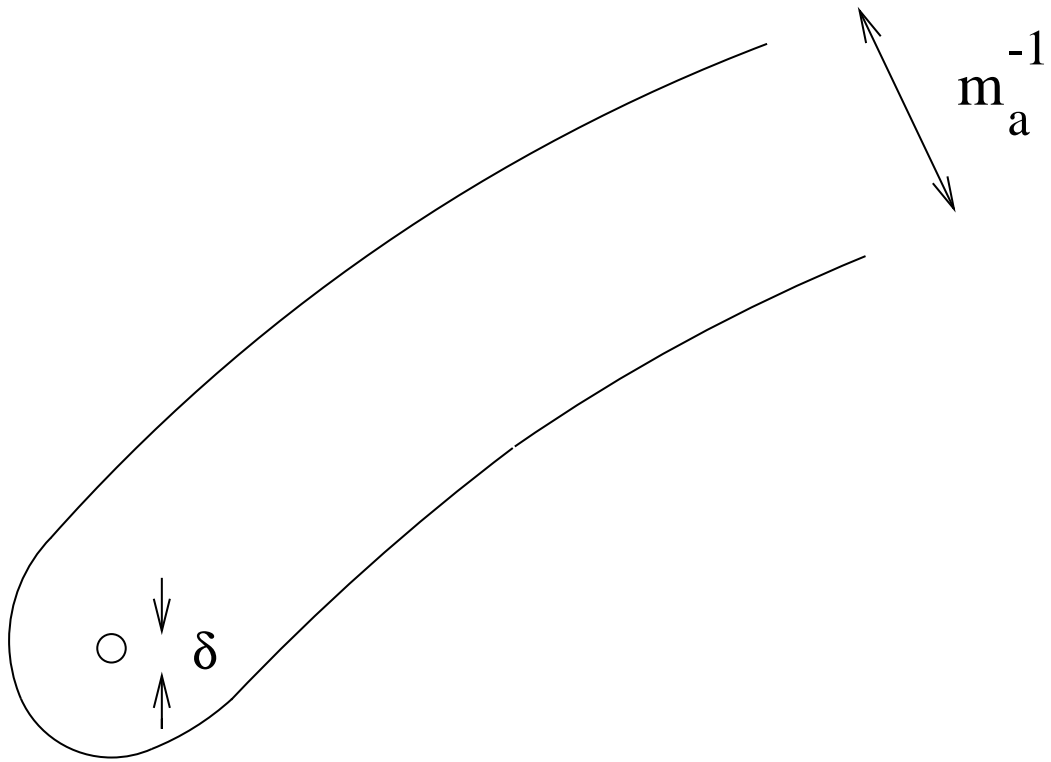


FIG. 1. Cross-section of a piece of wall bounded by a string. The wall thickness is m_a^{-1} . The string core size is $\delta = 1/\sqrt{\lambda v_a}$.

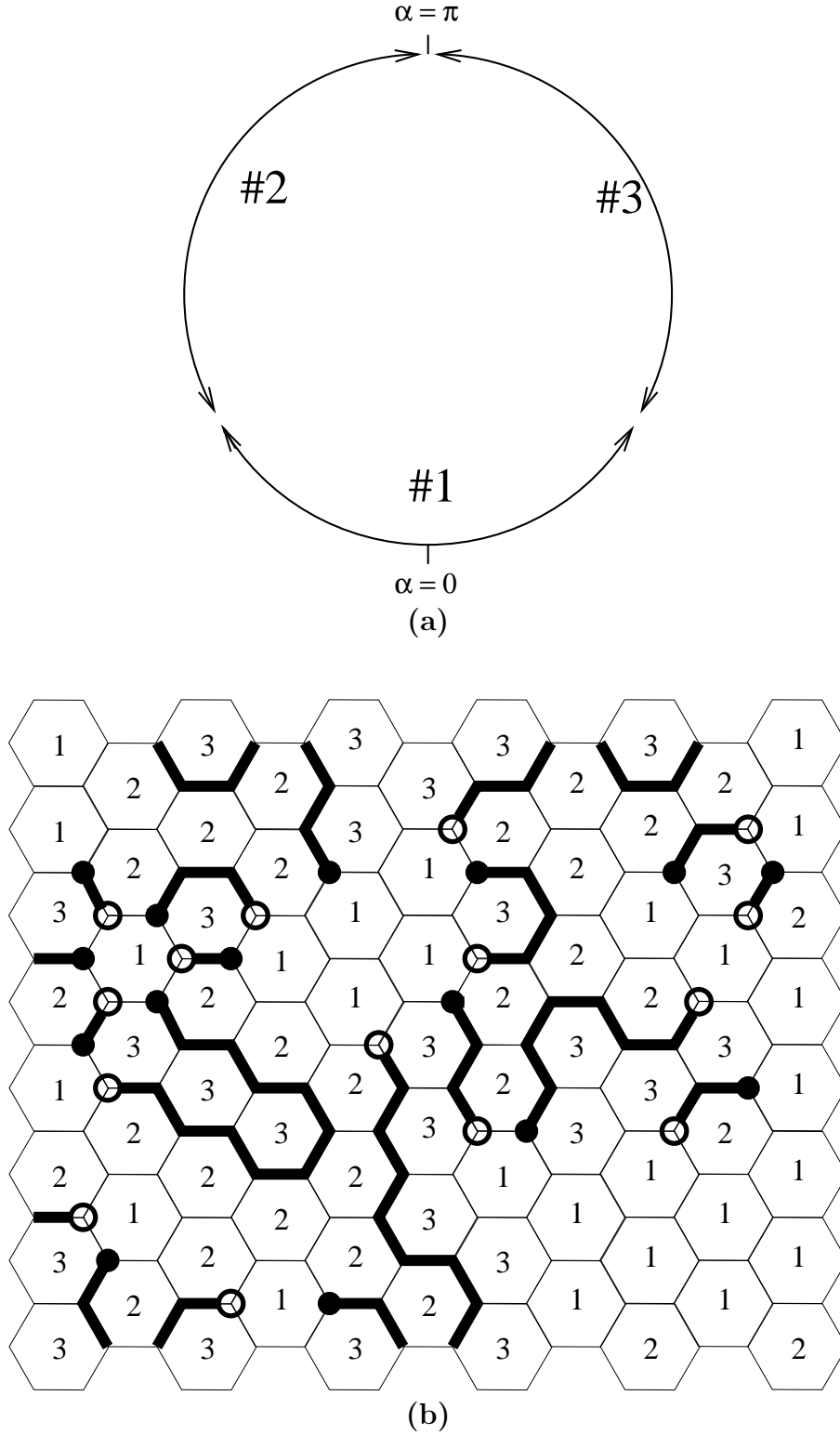


FIG. 2. (a) The circle of axion field expectation values is divided into three equal parts with the CP conserving value $\alpha = 0$ in the middle of part 1. (b) Each cell of a hexagonal grid is randomly assigned 1,2 or 3. This results in a set of domain walls (thick lines), upgoing strings (open circles), and downgoing strings (filled circles), as described in the text.

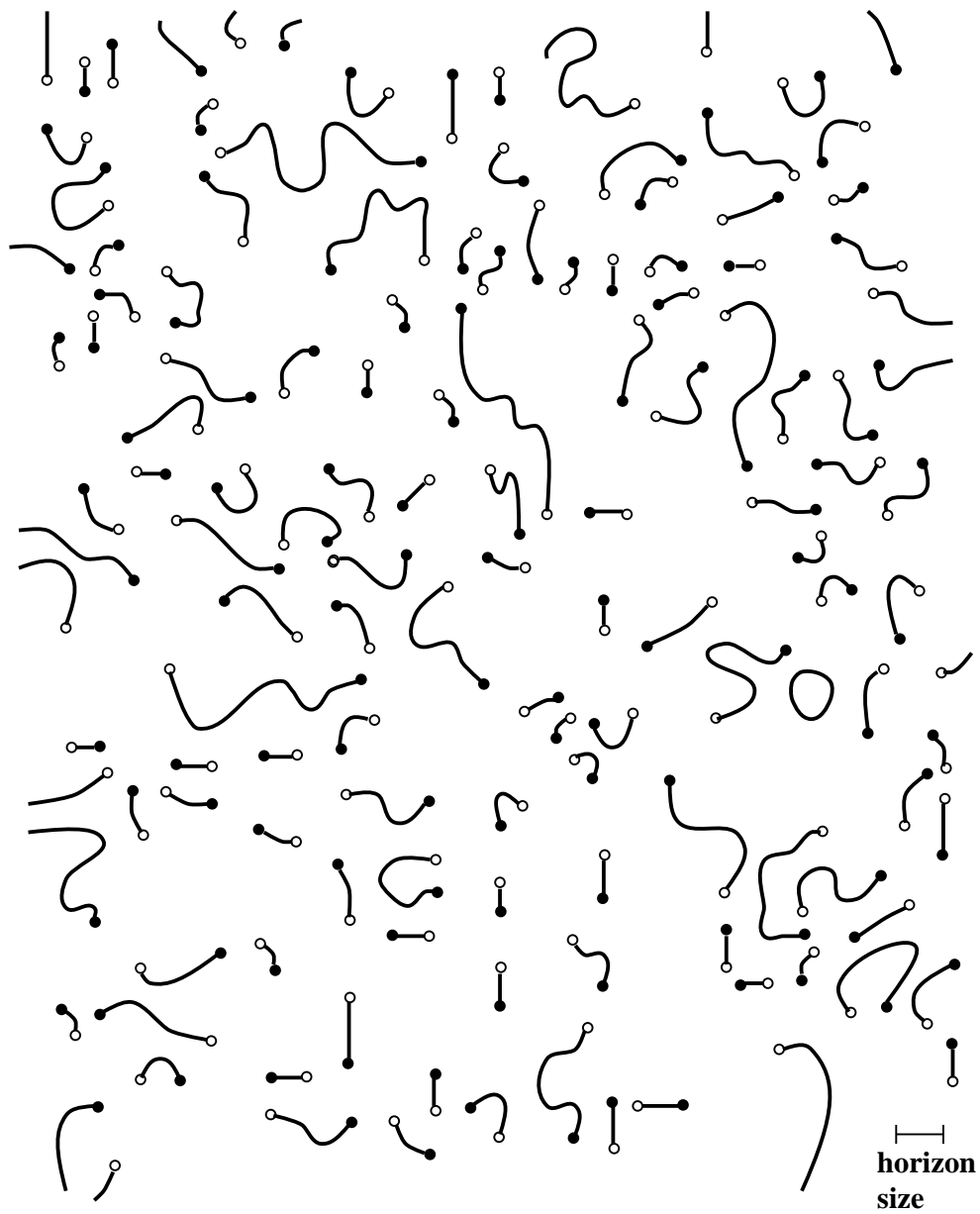


FIG. 3. Same as in Fig. 2b except that the area covered is larger, the underlying grid has been removed and the walls have been smoothed.

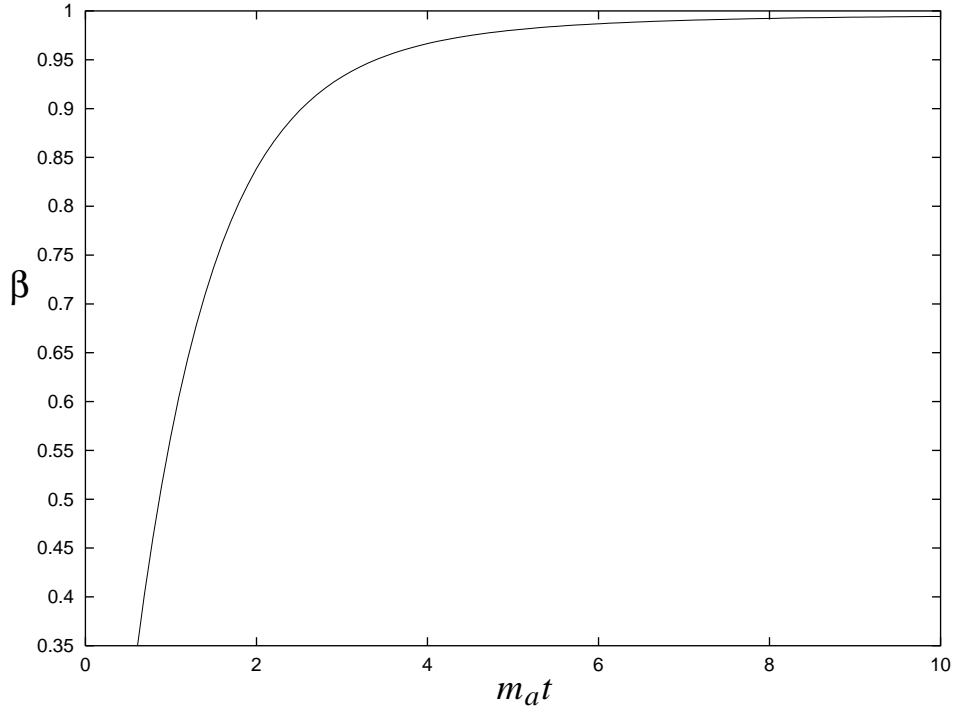


FIG. 4. Speed of the string core as a function of time for the case $1/m_a = 400$, $\sqrt{\lambda}/m_a = 10$, and $v = 0$.

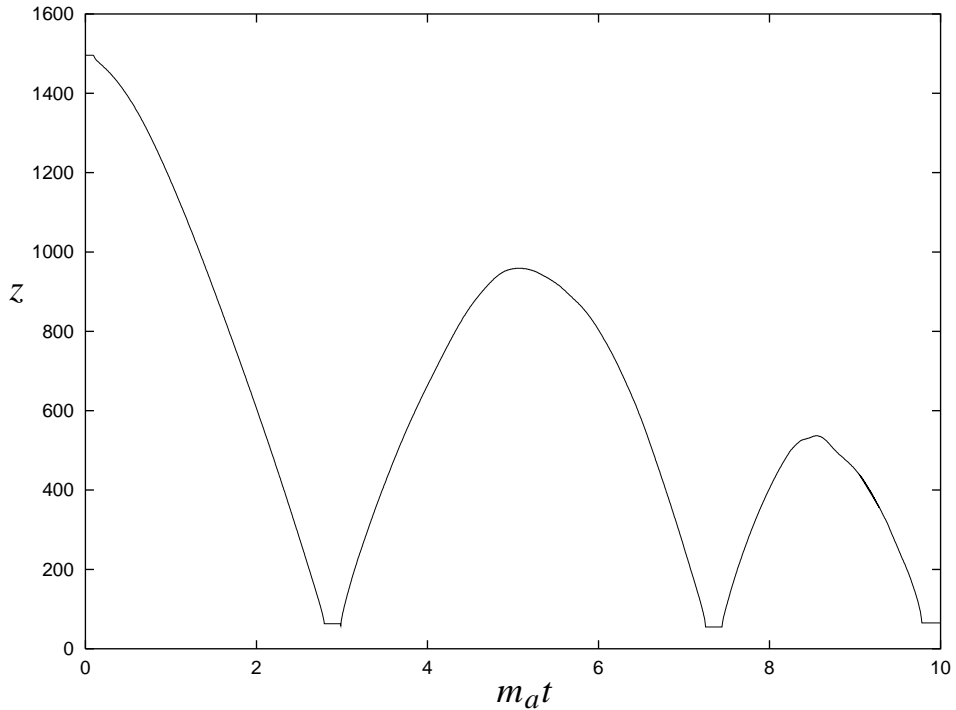
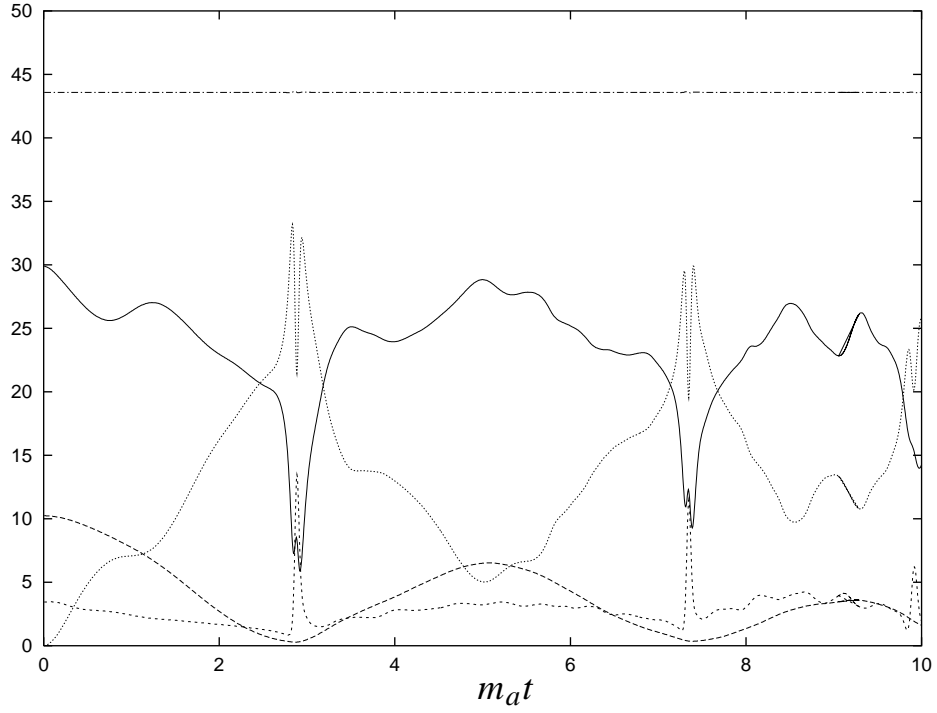
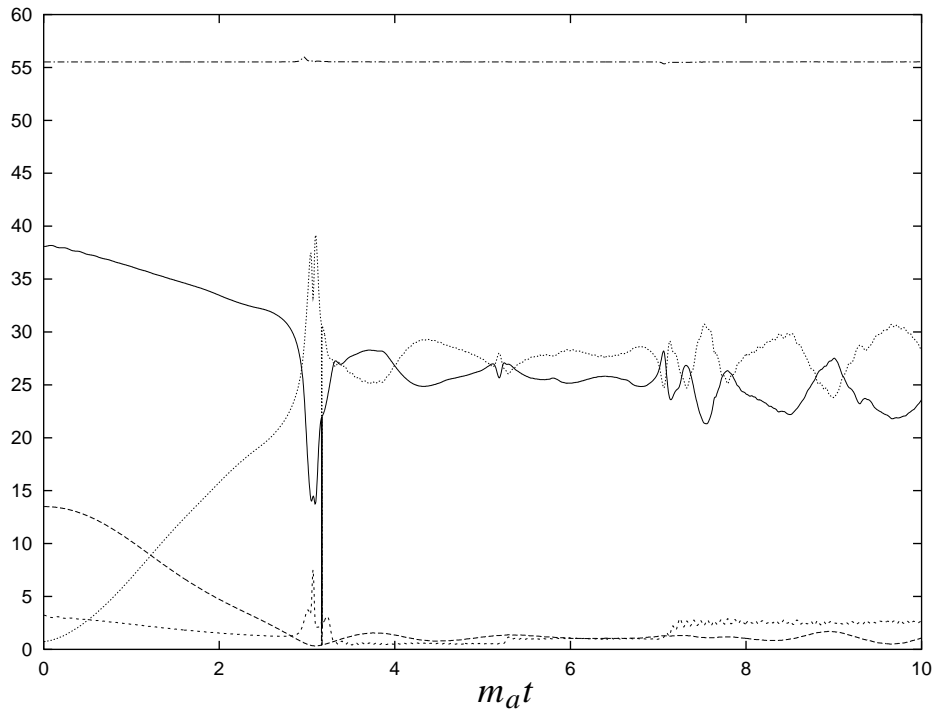


FIG. 5. Position of the string or anti-string core as a function of time for $1/m_a = 1000$, $\lambda = 0.0002$, $D = 2896$, and $v = 0$. The string and anti-string cores have opposite z . They go through each other and oscillate with decreasing amplitude.



(a)



(b)

FIG. 6. Gradient (solid), kinetic (dotted), wall potential (long dash), string potential (short dash) and total (dot dash) energy as a function of time for the case $1/m_a = 1000$, $\lambda = 0.0002$, $D = 2896$, and $v = 0$ (a), and for the case $1/m_a = 500$, $\lambda = 0.0032$, $D = 2096$ and $v = 0.25$ (b).

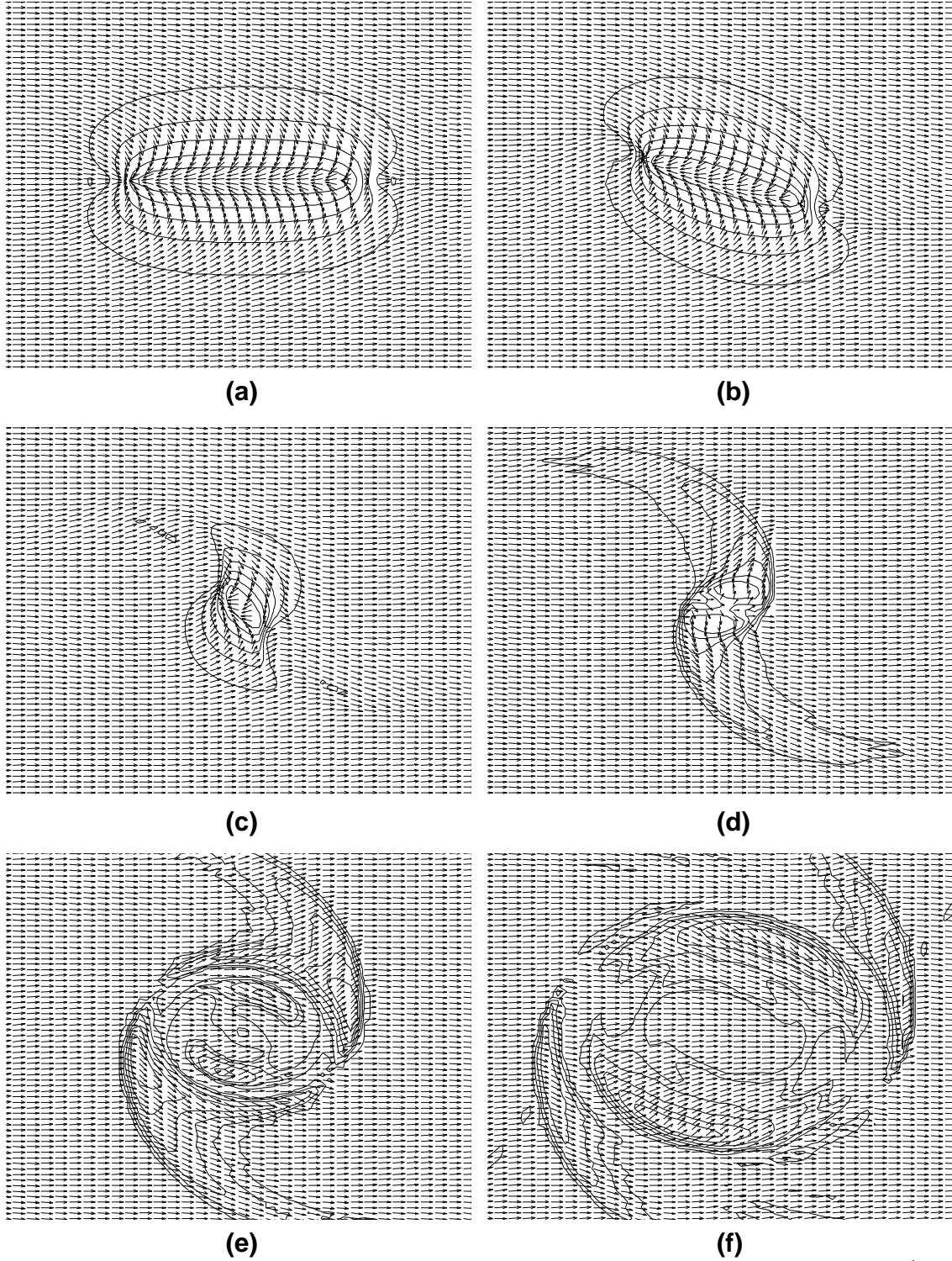


FIG. 7. Decay of a wall at successive time intervals $\Delta t = 1.2/m_a$ for the case $m_a^{-1} = 100$, $\lambda = 0.01$, $D = 524$, and $v = 0.6$.

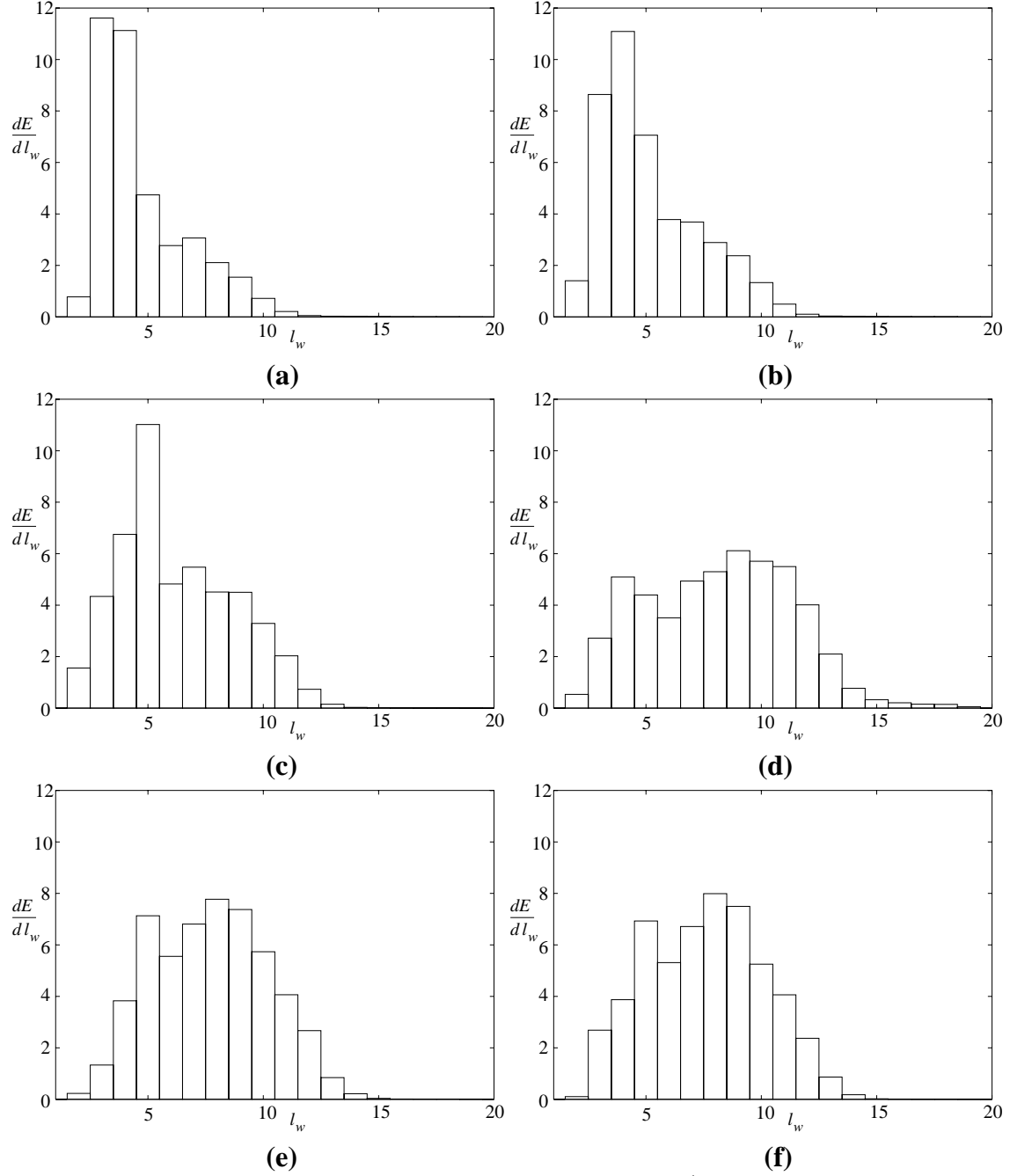


FIG. 8. Energy spectrum at successive time intervals $\Delta t = 1/m_a$, with $l_w = 18 \log(w/m_a)/\log(w_{\max}/m_a) + 2$ and $w_{\max} = \sqrt{8 + m_a^2}$, for the case $m_a^{-1} = 500$, $\lambda = 0.0032$, $D = 2096$ and $v = 0.25$.

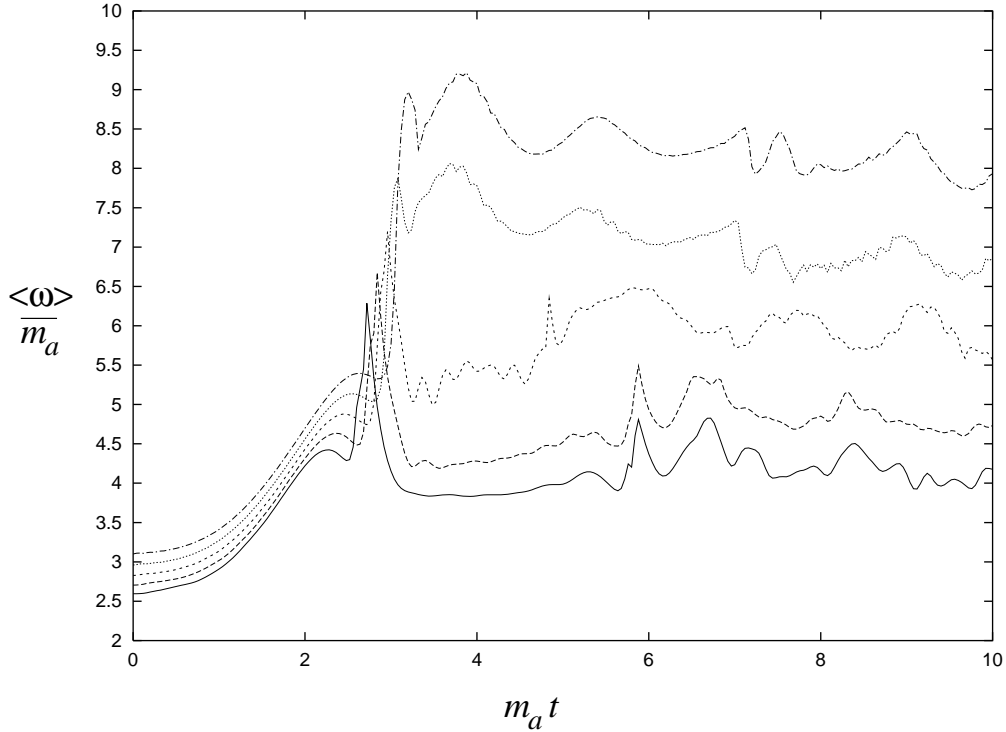


FIG. 9. $\langle \omega \rangle$ as a function of time for $1/m_a = 500$, $D = 2096$, $v = 0.25$ and $\lambda = 0.0004$ (solid), 0.0008 (long dash), 0.0016 (short dash), 0.0032 (dot) and 0.0064 (dot dash). After the wall has decayed, $\langle \omega \rangle$ is the average energy of radiated axions.

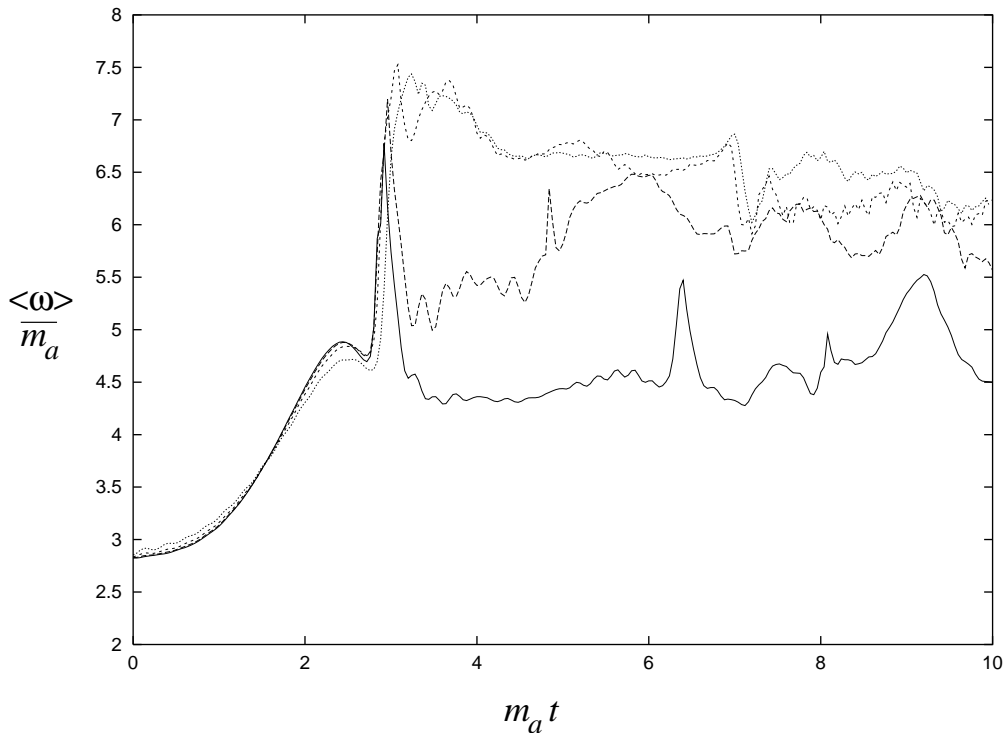


FIG. 10. Same as in Fig. 9 except $\lambda = 0.0016$, and $v = 0.15$ (solid), 0.25 (long dash), 0.4 (short dash) and 0.6 (dot).